FG.

NSWC/WOL/TR 75-195

12

AD A024511

NSWC/WOL/TR 75-195

NSWC TECHNICAL REPORT

WHITE OAK LABORATORY

NORMAL IMPINGEMENT OF A SUPERSONIC JET ON A PLANE — A BASIC STUDY OF SHOCK-INTERFERENCE HEATING

BY
Kuei-Yuan Chien

20 DECEMBER 1975

NAVAL SURFACE WEAPONS CENTER
WHITE OAK LABORATORY
SILVER SPRING, MARYLAND 20910

NAVAL SURFACE WEAPONS CENTER
WHITE OAK, SILVER SPRING, MARYLAND 20910

UNCLASSIFIED

SECURITY CLASSIFICATION OF THIS PAGE (When Data Entered)

REPORT DOCUMENTATION PAGE

READ INSTRUCTIONS BEFORE COMPLETING FORM

1. REPORT NUMBER (14) NSWC/WOL/TR-75-195	2. GOVT ACCESSION NO.
3. RECIPIENT'S CATALOG NUMBER (9) Technical rept.	
4. TITLE (and Subtitle) (6) NORMAL IMPINGEMENT OF A SUPERSONIC JET ON A PLANE - A BASIC STUDY OF SHOCK-INTERFERENCE HEATING.	5. TYPE OF REPORT & PERIOD COVERED
	6. PERFORMING ORG. REPORT NUMBER
7. AUTHOR(s) (10) Kuei-Yuan Chien	8. CONTRACT OR GRANT NUMBER(s)
9. PERFORMING ORGANIZATION NAME AND ADDRESS Naval Surface Weapons Center White Oak Laboratory White Oak, Silver Spring, Maryland 20910	10. PROGRAM ELEMENT, PROJECT, TASK AREA & WORK UNIT NUMBERS (16) A320-320C/WR023-02-003
11. CONTROLLING OFFICE NAME AND ADDRESS	12. REPORT DATE (11) 20 Dec [redacted] 75
	13. NUMBER OF PAGES 50
14. MONITORING AGENCY NAME & ADDRESS(if different from Controlling Office) (12) 53p.	15. SECURITY CLASS. (of this report) UNCLASSIFIED
	15a. DECLASSIFICATION/DOWNGRADING SCHEDULE

16. DISTRIBUTION STATEMENT (of this Report)

Approved for public release; distribution unlimited

17. DISTRIBUTION STATEMENT (of the abstract entered in Block 20, if different from Report)

18. SUPPLEMENTARY NOTES

19. KEY WORDS (Continue on reverse side if necessary and identify by block number)

Shock-Interference Heating
Supersonic Jet Impingement
Method of Integral Relations

20. ABSTRACT (Continue on reverse side if necessary and identify by block number)

The problem of a balanced, planar or axisymmetric, supersonic jet impinging normally on a flat surface has been considered based on an inviscid theory. The object of the study was to provide a rational model for calculating shock-interference heating as produced by a type IV shock-interaction pattern. The unwanted singularity at a low supersonic Mach number peculiar to scheme I of the one-strip formulation of the method of integral relations, over

DD FORM 1473, 1 JAN 73 EDITION OF 1 NOV 65 IS OBSOLETE
S/N 0102-014-6601

UNCLASSIFIED

SECURITY CLASSIFICATION OF THIS PAGE (When Data Entered)

391596 1b

as observed by South and by Gummer and Hunt, was successfully removed by the application of the scheme III of the one-strip formulation of the method of integral relations. The resulting simultaneous nonlinear algebraic equations were easily solved iteratively by the Newton-Raphson method. Sensitivity of the solution on various approximating functions employed was extensively investigated. Unlike the findings reported by Gummer and Hunt, solutions that satisfy all well-posed boundary conditions can be obtained by the one-strip formulation. Results indicate that, for the planar case, a rational engineering solution for the stagnation-point velocity gradient (and hence the peak heat-transfer rate) has been obtained. For the axisymmetric case, however, solutions appear to be not quite converging. A two-strip formulation based on the method of integral relations is also included.

 20 December 1975

NORMAL IMPINGEMENT OF A SUPERSONIC JET ON A PLANE - A BASIC STUDY OF SHOCK-INTERFERENCE HEATING

This report presents a theoretical method to predict the severity of shock-interference heating caused by the impingement of a shock wave on a blunt fin. The problem of a supersonic jet (resulting from the interaction of the incident shock with the fin bow shock) impinging on the fin surface was studied based on the one-strip formulation of the method of integral relations. A rational engineering solution for the stagnation-point velocity gradient (and hence the peak heat-transfer rate) has been obtained for the planar case. The present jet-impingement model could be coupled with the shock-interference model of Edney to predict type IV shock-interaction effects.

The present study was sponsored by the Naval Air Systems Command, AIR-320C, under Air Task No. A320-320C/WR023-02-003.

Kurt R. Enkenhus

KURT R. ENKENHUS
By direction

CONTENTS

TABLES

ILLUSTRATIONS

SYMBOLS

a	speed of sound
E	specific entropy function, p/ρ^{γ}
j	equal to zero (planar case) or one (axisymmetric case)
M	Mach number
p	static pressure
q	total speed, $(u^2 + v^2)^{1/2}$
r	coordinate axis along the plate surface
u	velocity component in the r-direction
v	velocity component in the y-direction
V_∞	free-stream velocity of the jet
y	coordinate axis perpendicular to the plate surface
β	constant, $(\gamma - 1)/2\gamma$
γ	ratio of (constant) specific heats
δ	the angle the upper boundary of the wall jet makes with respect to the negative y-direction (see Fig. 1)
ε	detachment distance of the shock wave or of the wall-jet boundary (see Fig. 1)
η	location of the sonic point at the wall
θ	the angle the flow behind the shock wave makes with respect to the negative y-direction
ρ	density
σ	the angle the shock wave makes with respect to the negative y-direction (see Fig. 1)
GMC	method that employs the equation of global mass conservation, Eq. (41)
MCE	method that employs the equation of modified continuity, Eq. (7)
PWS	method that employs piecewise smooth approximating functions

SYMBOLS (Cont'd)

SP method that imposes the condition of satisfying Eq. (56) at $r = 0$

Subscripts

- j at the upper boundary of the wall jet
- s at the shock wave
- w at the plate surface
- η at the surface sonic point
- 0 at $r = 0$
- 1 at the line of the jet edge, $r = 1$
- 2 at $r = 1/2$
- ∞ at free stream

INTRODUCTION

As an extraneous shock wave impinges on a blunt body in a hypersonic flow, greatly increased aerodynamic heating and pressure over a very small region near the impingement point have been observed (Refs. (1) to (5)). The incident shock wave may be generated either by boundary-layer separation (Refs. (3) to (5)) or

---

(1) Edney, B., "Anomalous Heat Transfer and Pressure Distributions on Blunt Bodies at Hypersonic Speeds in the Presence of an Impinging Shock," FFA Report 115, The Aeronautical Research Institute of Sweden, Stockholm, 1968

(2) Hains, F. D. and Keyes, J. W., "Shock Interference Heating in Hypersonic Flows," AIAA Journal, Vol. 10, 1972, pp. 1441-1447

(3) Hiers, R. S. and Loubsky, W. J., "Effects of Shock-Wave Impingement on the Heat Transfer on a Cylindrical Leading Edge," NASA TN D-3859, Ames Research Center, Moffett Field, Calif., 1967

(4) Kaufman, L. G., III, Korkegi, R. H. and Morton, L. C., "Shock Impingement Caused by Boundary Layer Separation Ahead of Blunt Fins," ARL TR 72-0118, Aerospace Research Laboratories, WPAFB, Ohio, 1972

(5) Gillerlain, J. D., Jr., "Experimental Investigation of a Fin-Cone Interference Flow Field at Mach 5," NSWC/WOL/TR 75-63 Naval Surface Weapons Center, White Oak Lab., Silver Spring, Md., 1976

by an extraneous surface (Refs. (1) to (3)). Six different types of shock-interaction patterns have been classified by Edney based on an extensive experimental study (Ref. (1)). Among them, the type IV interference pattern produces the most severe shock-interference heating and pressure. This interference results in a supersonic jet embedded in the subsonic flow field. In fact, peak interference heating rates up to 17 times the interference-free stagnation-point value and peak pressures up to eight times the free-stream pitot pressure level have been measured by Hains and Keyes (Ref. (2)).

Despite its significance, past analyses (Refs. (1) to (3) and (6)) on the type IV interference were inadequate and generally empirical in nature. Recently, a time-dependent finite-difference method was used by Tannehill, Holst and Rakich (Ref. (7)) to solve the Navier-Stokes equations for the two-dimensional shock-impingement problem. Although, in principle, their computer program can be used to compute all six types of shock interactions, only type III interference results have been published so far. However, the elaborate computations involved and the extensive computer time required by their method make it highly desirable to have some relatively simple, yet reasonably accurate, approximate method. Such an approach has in fact been pursued by Edney (Ref. (1)) and by Keyes and Hains (Ref. (6)). However, their empirical treatments of the jet-impingement process suggest the need for a more rational study. This is the subject of the present paper.

The impingement of a balanced supersonic jet on a flat surface was studied both theoretically and experimentally for an axisymmetric jet at normal impingement by Gummer and Hunt (Ref. (8)), and theoretically for a plane jet at an arbitrary angle with the surface by Bukovshin and Shestova (Ref. (9)). Both groups have used the scheme I of the method of integral relations in its crudest form (one strip) (Ref. (10)). However, in both studies the centered

---

(6) Keyes, J. W. and Hains, F. D., "Analytical and Experimental Studies on Shock Interference Heating in Hypersonic Flows," NASA TN D-7139, Langley Research Center, Hampton, Va., 1973

(7) Tannehill, J. C., Holst, T. L. and Rakich, J. V., "Numerical Computation of Two-Dimensional Viscous Blunt Body Flows with an Impinging Shock," AIAA Paper 75-154, AIAA 13th Aerospace Sciences Meeting, 20-22 Jan 1975

(8) Gummer, J. H. and Hunt, B. L., "The Impingement of a Uniform, Axisymmetric, Supersonic Jet on a Perpendicular Flat Plate," The Aeronautical Quarterly, Vol. XXII, Part 4, 1971, pp. 403-420

(9) Bukovshin, V. G. and Shestova, N. P., "Incidence of Plane Supersonic Jet on a Plane at an Arbitrary Angle," Fluid Dynamics, Vol. 2, No. 4, 1967, pp. 97-100

(10) Belotserkovskii, O. M., ed., "Supersonic Gas Flow Around Blunt Bodies," NASA Technical Translation TTF-453, June 1967

expansion to ambient pressure of the jet-edge streamline behind the shock wave was not properly considered, and instead an empirical condition of sonic velocity at the jet edge behind the shock wave was imposed. Furthermore, at low supersonic Mach numbers, both South (Ref. (11)) and Gummer and Hunt (Ref. (8)) have pointed out the singular behavior of the governing equation of the scheme I of the method of integral relations. This singularity, which has no counterpart in an exact solution, will cause the computation in the shock layer to break down. This is of special importance to us since, according to Edney (Ref. (1)), low supersonic Mach numbers are in the range of particular interest to the shock-interference problem.

The singularity can be shown to be easily removed if the governing differential equations are integrated once again along the body-surface direction. This constitutes the scheme III of the method of integral relations (Ref. (10)). This approach was utilized in the present study to generate solutions to the one-strip approximation equations of the jet-impingement problem. As we shall show later, in contrast to the findings reported by Gummer and Hunt (Ref (8)), the one-strip approximation does yield solutions that satisfy all well-posed boundary conditions. A two-strip formulation of the problem has also been completed, but solutions have not yet been carried out. For the sake of completeness, this is included in the Appendix.

PROBLEM FORMULATION

GOVERNING EQUATIONS

Consider the flow geometry schematically shown in Figure 1. The origin of the coordinate system is placed at the stagnation point of the flat surface. The problem is considered to be steady and two-dimensional or axisymmetric, with r and y axes along and perpendicular to the plate surface, respectively, and the free-stream jet flow is in the negative y-direction. For simplicity, the gas is assumed to be inviscid and obeys the perfect gas law; its conditions are characterized by the pressure, p, density, ρ, temperature, T, and velocity components, u and v, in the r and y directions, respectively. Ahead of the shock wave, the jet is assumed to be uniform with constant static pressure equal to the ambient value. These assumptions are of the usual kind that are generally made by other investigators. Heat-transfer rates can be calculated using the well-known boundary-layer results once the pressure distribution along the plate surface is determined from the inviscid approach.

(11) South, J. C., Jr., "Calculation of Axisymmetric Supersonic Flow Past Blunt Bodies with Sonic Corners, Including a Program Description and Listing," NASA TN D-4563, Langley Research Center, Hampton, Va., 1968

Under these conditions, the governing conservation equations are

$$\frac{\partial}{\partial r}(r^j \rho u) + \frac{\partial}{\partial y}(r^j \rho v) = 0 \quad (1)$$

$$\frac{\partial}{\partial r}(r^j \rho uv) + \frac{\partial}{\partial y}[r^j (\beta p + \rho v^2)] = 0 \quad (2)$$

$$\frac{\partial}{\partial r}[r^j (\beta p + \rho u^2)] + \frac{\partial}{\partial y}(r^j \rho uv) = j\beta p \quad (3)$$

and

$$p = \rho(1 - q^2) \quad (4)$$

where

$$\beta = \frac{(\gamma - 1)}{2\gamma}$$

$$q^2 = u^2 + v^2$$

$j = 0$ or 1 for two-dimensional or axisymmetric jets, respectively, and γ is the ratio of (constant) specific heats. The variables are all nondimensional. Thermodynamic variables are nondimensionalized by the corresponding stagnation values in the free-stream jet, velocities by the maximum adiabatic velocity and distance by the jet radius. Obviously, the magnitude of the nondimensional free-stream jet velocity is related to the free-stream jet Mach number by

$$V_\infty = \left[\frac{(\gamma - 1)M_\infty^2}{2 + (\gamma - 1)M_\infty^2}\right]^{1/2}$$

There is also a geometric relation

$$\frac{d\varepsilon}{dr} = - \cot \sigma \quad (5)$$

in the shock layer, and

$$\frac{d\varepsilon}{dr} = - \cot \delta \quad (6)$$

in the wall-jet layer, where ε is the detachment distance of the shock wave or of the wall jet, σ and δ are the angles the shock wave and the upper boundary of the wall jet make with respect to the free-stream jet flow direction, respectively (see Fig. 1).

The method of integral relations requires that the governing partial differential equations be cast into divergence form, such as Equations (1) to (3). However, combinations of these equations can also be represented in divergence form. For example, one may combine the relation of constant entropy along streamlines, the energy equation (4), and the continuity equation (1) to yield a modified continuity equation

$$\frac{\partial}{\partial r}\left[r^j u(1 - q^2)^{1/(\gamma-1)}\right] + \frac{\partial}{\partial y}\left[r^j v(1 - q^2)^{1/(\gamma-1)}\right] = 0 \qquad (7)$$

which was the original, widely employed formulation of Belotserkovskii (Ref. (12)). For a sphere in supersonic flow, Xerikos and Anderson (Ref. (13)) found that the one-strip formulation based on the modified continuity equation yielded results which agree with experiments better than that based on the original continuity equation. The difference is expected to disappear when the number of strips increases. In the present one-strip formulations, however, Equation (7) will be used instead of Equation (1).

An additional simplification arises when only one strip is used in the formulation, namely, the strip boundaries are either the shock wave or streamlines. Along the plate surface, the constant entropy relationship can be used to relate pressure to the surface velocity. This algebraic relation can thus be employed to replace the radial momentum equation (3), as we shall see in the next section.

The flow field can be divided into two regions, a shock-layer region ($0 \leq r \leq 1$) and a wall-jet region ($1 \leq r \leq \eta$), where $r = \eta$ is the location of the sonic point at the wall

$$u_w(\eta) = a_w(\eta)$$

and it is unknown, a priori. The two regions are related by the requirements that, at $r = 1$, ε, E and ψ are continuous and σ and δ are governed by the Prandtl-Meyer expansion relation, where E is the specific entropy function

$$E = p/\rho^\gamma$$

and ψ is the stream function. If θ is the angle the flow behind the shock wave makes with respect to the negative y-direction, then the oblique shock relations give

$$\cot \theta_1 = \left[\frac{(\gamma + 1)M_\infty^2}{2(M_\infty^2 \sin^2\sigma_1 - 1)} - 1\right] \tan \sigma_1 \qquad (8)$$

---

(12) Belotserkovskii, O. M., "Flow With a Detached Shock Wave About a Symmetrical Profile," Journal of Applied Mathematics and Mechanics, Vol. 22, 1958, pp. 279-296

(13) Xerikos, J. and Anderson, W. A., "An Experimental Investigation of the Shock Layer Surrounding a Sphere in Supersonic Flow," AIAA Journal, Vol. 3, 1965, pp. 451-457

where the subscript 1 denotes quantities evaluated at $r = 1$. Now, δ_1 is related to θ_1 by

$$\delta_1 = \theta_1 + \left(\frac{\gamma + 1}{\gamma - 1}\right)^{1/2} \left\{\tan^{-1}\left[\left(\frac{\gamma - 1}{\gamma + 1}\right)(M_j^2 - 1)\right]^{1/2} - \tan^{-1}\left[\left(\frac{\gamma - 1}{\gamma + 1}\right)(M_{s1}^2 - 1)\right]^{1/2}\right\} - \left\{\tan^{-1}(M_j^2 - 1)^{1/2} - \tan^{-1}(M_{s1}^2 - 1)^{1/2}\right\} \tag{9}$$

where

$$M_j^2 = \frac{2\rho_j q_j^2}{(\gamma - 1)p_j} = \frac{2q_j^2}{(\gamma - 1)(1 - q_j^2)}$$

and

$$M_{s1}^2 = \frac{2q_{s1}^2}{(\gamma - 1)(1 - q_{s1}^2)}$$

The subscripts j and s denote, respectively, quantities evaluated at the upper boundary of the wall jet and right behind the shock wave. Obviously,

$$p_j = p_\infty = \left[1 + \frac{(\gamma - 1)M_\infty^2}{2}\right]^{-\gamma/(\gamma-1)} \tag{10}$$

$$\rho_j = (p_j/E_j)^{1/\gamma} \tag{11}$$

$$E_j = E_{s1} \tag{12}$$

and

$$q_j = (1 - p_j/\rho_j)^{1/2} \tag{13}$$

The specific entropy function evaluated right behind the shock at $r = 1$, E_{s1}, depends only on M_∞, γ and σ_1. Hence, from Equations (8) to (13), we obtain

$$\delta_1 = \text{fun}(M_\infty, \gamma, \sigma_1)$$

Since the upper boundary of the wall-jet layer, $y = \varepsilon(r)$ for $r \geq 1$, is a streamline, we have

$$\frac{d\varepsilon}{dr} = \frac{v_j}{u_j} = -\cot\delta \tag{14}$$

For δ in the first two quadrants only, we may combine Equations (4) and (14) to yield

$$u_j = q_j \sin\delta \tag{15}$$

$$v_j = -q_j \cos\delta \tag{16}$$

The signs are determined from the fact that $u_j \geq 0$ for $r \geq 1$. The boundary conditions are:

A. At the wall, $y = 0$

$$v_w = 0 \tag{17}$$

$$E_w = E_{s0} \tag{18}$$

where E_{s0} is the specific entropy function evaluated right behind the shock at $r = 0$.

B. At the centerline, $r = 0$

$$u = 0 \tag{19}$$

$$E = E_{s0} \tag{20}$$

$$\sigma = \pi/2 \tag{21}$$

C. At the shock wave, $y = \varepsilon(r)$, $r \leq 1$, the Rankine-Hugoniot relations for the gas apply:

$$u_s = V_\infty\left[\frac{2\cot\sigma}{(\gamma+1)M_\infty^2}\left(M_\infty^2\sin^2\sigma - 1\right)\right] \tag{22}$$

$$v_s = V_\infty\left[\frac{2(M_\infty^2\sin^2\sigma - 1)}{(\gamma+1)M_\infty^2} - 1\right] \tag{23}$$

$$\rho_s = \left[1 + \frac{(\gamma-1)M_\infty^2}{2}\right]^{-1/(\gamma-1)}\left[\frac{(\gamma+1)M_\infty^2\sin^2\sigma}{2 + (\gamma-1)M_\infty^2\sin^2\sigma}\right] \tag{24}$$

$$E_s = \left[\frac{2\gamma M_\infty^2 \sin^2\sigma - (\gamma - 1)}{(\gamma + 1)}\right]\left[\frac{2 + (\gamma - 1)M_\infty^2 \sin^2\sigma}{(\gamma + 1)M_\infty^2 \sin^2\sigma}\right]^\gamma \tag{25}$$

$$p_s = E_s \rho_s^\gamma \tag{26}$$

D. At the jet boundary, $y = \varepsilon(r)$, $r \geq 1$, Equations (8) to (16) apply.

METHOD OF INTEGRAL RELATIONS - SCHEME I

A. SHOCK-LAYER REGION. Integrating the axial momentum equation (2) from 0 to ε, and utilizing the identity that

$$\int_0^{\varepsilon(r)} \frac{\partial}{\partial r}(r^j \rho uv)\,dy = \frac{d}{dr}\int_0^{\varepsilon(r)} r^j \rho uv\,dy - \frac{d\varepsilon}{dr} r^j \rho_s u_s v_s$$

we obtain

$$\frac{d}{dr}\int_0^{\varepsilon(r)} r^j \rho uv\,dy - \frac{d\varepsilon}{dr} r^j \rho_s u_s v_s + r^j\{\beta(p_s - p_w) + \rho_s v_s^2 - \rho_w v_w^2\} = 0 \tag{27}$$

In the first approximation, the integrand is assumed to be linear in y so that Equation (27) is approximated by

$$\frac{d}{dr}[r^j \varepsilon \rho_s u_s v_s] + 2r^j\{\beta(p_s - p_w) + \rho_s v_s(v_s + u_s \cot\sigma)\} = 0 \tag{28}$$

Equations (5) and (17) have been used in the above equation. Similarly, Equation (7) can be integrated over the thickness of the shock layer to yield

$$\frac{d}{dr}\left\{r^j \varepsilon\left[u_s(1 - q_s^2)^{1/(\gamma-1)} + u_w(1 - u_w^2)^{1/(\gamma-1)}\right]\right\}$$
$$+ 2r^j(1 - q_s^2)^{1/(\gamma-1)}[v_s + u_s \cot\sigma] = 0 \tag{29}$$

From Equations (4) and (18) and the definition of the specific entropy function, we obtain the algebraic relation that

$$p_w = \left[\frac{(1 - u_w^2)^\gamma}{E_{s0}}\right]^{1/(\gamma-1)} \tag{30}$$

Since, for fixed values of M_∞ and γ, the quantities evaluated at the shock depend only on σ (as can be seen from the Rankine-Hugoniot relations), Equations (5), (28) and (29) are the governing equations for the variables ε, σ and u_w. This constitutes the scheme I of the method of integral relations. Initial conditions are Equations (19) and (21). It is well known in related blunt-body problems that the missing third initial condition is supplied by the regularity condition at the surface sonic point (Refs. (10) to (12)). For the jet-impingement problem, this requires the consideration of the wall jet since the surface sonic point lies outside the shock layer (Ref. (8)). Before we proceed any further, it is important to point out a singular feature of the scheme I formulation. The singularity occurs as

$$\frac{d(\rho_s u_s v_s)}{d\sigma} = 0$$

in Equation (28) and $\frac{d\sigma}{dr}$ becomes unbounded. This has no counterpart in an exact solution. As was remarked by South (Ref. (11)) and by Gummer and Hunt (Ref. (8)), the singularity occurs in the shock layer for $M_\infty \sim 2$. In fact, Gummer and Hunt found no solution that will satisfy the wall-jet relations. Since $\frac{d(\rho_s u_s v_s)}{d\sigma}$ will appear in any method that approximates the integral in Equation (27) by an end-point quadrature formula, this singularity is peculiar to scheme I of the method of integral relations and cannot be removed by utilizing multi-strip formulations, although the particular Mach number at which the singularity occurs might be different from that of the one-strip formulation. If, on the other hand, the governing ordinary differential equations are integrated again in the r-direction, the singularity disappears since we now have algebraic equations. This is the scheme III of the method of integral relations, which will be discussed after we complete our consideration of the wall-jet region in the scheme I formulation.

B. <u>WALL-JET REGION</u>. Integrating Equations (2) and (7) from the plate to the upper boundary of the wall jet, we obtain

$$\frac{d}{dr}[r^j \varepsilon \rho_j u_j v_j] + 2r^j \beta (p_j - p_w) = 0 \tag{31}$$

and

$$\frac{d}{dr}\left\{r^j \varepsilon \left[u_j (1 - q_j^2)^{1/(\gamma-1)} + u_w (1 - u_w^2)^{1/(\gamma-1)}\right]\right\} = 0 \tag{32}$$

Because of Equation (14), these governing equations are considerably simpler than the corresponding ones in the shock layer. Utilizing Equations (15), (16) and (30), one can conclude that Equations (14), (31) and (32) are the governing equations for the variables ε, δ and u_w. Initial conditions are, at $r = 1$

$$\varepsilon = \varepsilon_1$$

$$u_w = u_{w1}$$

$$\delta = \delta_1$$

The first two are supplied by the shock-layer solution, and the third by using Equation (9) and the shock-layer solution.

Note that

$$\frac{d}{dr}\left[u_w(1 - u_w^2)^{1/(\gamma-1)}\right] = (1 - u_w^2)^{(2-\gamma)/(\gamma-1)}\left[1 - \left(\frac{\gamma + 1}{\gamma - 1}\right)u_w^2\right]\frac{du_w}{dr}$$

Equation (32) becomes singular as

$$u_w = \left(\frac{\gamma - 1}{\gamma + 1}\right)^{1/2} \equiv u_{w\eta} \tag{33}$$

Utilizing the energy equation and the definition of the speed of sound

$$a = \left[\frac{(\gamma - 1)p}{2\rho}\right]^{1/2} \tag{33a}$$

one may show that Equation (33) implies that

$$u_w = a_w \tag{33b}$$

Therefore, the singular point is the surface sonic point, $r = \eta$. Since the wall velocity at $r = \eta$ is continuous for a smooth plate, we may impose the regularity condition that, at $r = \eta$

$$\left[1 + \csc\delta_\eta(1 - \cot^2\delta_\eta)\,\frac{u_{w\eta}(1 - u_{w\eta}^2)^{1/(\gamma-1)}}{q_j(1 - q_j^2)^{1/(\gamma-1)}}\right]\left(\frac{j\varepsilon_\eta}{\eta} - \cot\delta_\eta\right)$$

$$- 2\beta\cot\delta_\eta\csc^2\delta_\eta\frac{(p_j - p_{w\eta})}{\rho_j q_j^2} = 0 \tag{34}$$

so that $\frac{du_w}{dr}$ is finite there. The subscript η denotes quantities evaluated at $r = \eta$. Equation (34), derived after some tedious but straightforward algebra from Equations (31) and (32), provides the missing initial condition of the shock-layer equations. This completes the formulation of the scheme I of the method of integral relations.

METHOD OF INTEGRAL RELATIONS - SCHEME III

Since Gummer and Hunt (Ref. (8)) could not find solutions that will satisfy the wall-jet equations by the scheme I of the method of integral relations, and since they and South (Ref. (11)) have pointed out the singular behavior of Equation (28) for low supersonic Mach numbers, the scheme III of the method of integral relations is used in the present study. Two different formulations have been considered and they will be discussed in the following.

A. ONE-BY-TWO SOLUTION. Consider first the simplest case that the flow field between $r = 0$ and $r = \eta$ is divided into two zones: $0 \le r \le 1$ and $1 \le r \le \eta$. Consider, in the shock layer, the simplest approximation

$$-\frac{d\varepsilon}{dr} = \cot\sigma \simeq r\cot\sigma_1 \tag{35}$$

which can be integrated to yield

$$\varepsilon = \varepsilon_0 - \frac{r^2\cot\sigma_1}{2} \tag{36}$$

where $\varepsilon_0 \equiv \varepsilon(r = 0)$. Equation (36) gives the relation between the shock distances and σ_1 as

$$\cot\sigma_1 = 2(\varepsilon_0 - \varepsilon_1) \tag{37}$$

Integrating Equation (28) from $r = 0$ to 1 and utilizing Equation (19), we obtain

$$\rho_{s1}u_{s1}v_{s1}\varepsilon_1 + 2\int_0^1 r^j\{\beta(p_s - p_w) + \rho_s v_s(v_s + u_s\cot\sigma)\}dr = 0 \tag{38}$$

The terms inside the curly brackets are even functions of r. Hence, we may use the simplest approximating function

$$f(r) \approx f_0 + (f_1 - f_0)r^2$$

and Equation (38) thus becomes

$$\rho_{s1}u_{s1}v_{s1}\varepsilon_1 + \frac{4}{(j+1)(j+3)}\left[\rho_{s0}v_{s0}^2 + \beta(p_{s0} - p_{w0})\right]$$
$$+ \frac{2}{(j+3)}[\rho_{s1}v_{s1}(v_{s1} + u_{s1}\cot\sigma_1) + \beta(p_{s1} - p_{w1})] = 0 \tag{39}$$

Obviously, Equation (39), being an algebraic equation, is nonsingular. Similar application of the simplest approximating function to Equation (29) yields

$$\varepsilon_1 \left[u_{s1}(1 - q_{s1}^2)^{1/(\gamma-1)} + u_{w1}(1 - u_{w1}^2)^{1/(\gamma-1)} \right]$$

$$+ \frac{4v_{s0}(1 - v_{s0}^2)^{1/(\gamma-1)}}{(j + 1)(j + 3)} + \frac{2(1 - q_{s1}^2)^{1/(\gamma-1)}}{(j + 3)} (v_{s1} + u_{s1}\cot\sigma_1) = 0 \quad (40)$$

We could use, instead of Equation (40), an equation of global mass conservation

$$\frac{\rho_\infty V_\infty}{(1 + j)} = \int_0^\varepsilon r^j \rho u dy \bigg|_{r=1} \approx \frac{\varepsilon_1}{2} (\rho_{s1}u_{s1} + \rho_{w1}u_{w1}) \quad (41)$$

Obviously, ρ_{w1} is related to u_{w1} by Equations (4) and (30) as

$$\rho_{w1} = \left[\frac{1 - u_{w1}^2}{E_{s0}} \right]^{1/(\gamma-1)}$$

Note that Equation (41) is independent of the approximating functions used in the radial direction. It depends only on the assumption of a linear variation of ρu with y, which is always the case for a one-strip formulation.

In the wall jet, $1 \leq r \geq \eta$, consider

$$- \frac{d\varepsilon}{dr} = \cot\delta \approx \frac{r}{\eta(1 - \eta^2)} [(1 - r^2)\cot\delta_\eta + \eta(r^2 - \eta^2)\cot\delta_1] \quad (42)$$

which yields, after a straightforward integration process

$$\varepsilon = \varepsilon_1 + \frac{(r^2 - 1)}{4\eta(1 - \eta^2)} [2(\eta^3\cot\delta_1 - \cot\delta_\eta)$$

$$+ (r^2 + 1)(\cot\delta_\eta - \eta\cot\delta_1)] \quad (43)$$

which gives the relation between ε_η and δ_η as

$$\varepsilon_\eta = \varepsilon_1 + \frac{(1 - \eta^2)}{4\eta} (\eta\cot\delta_1 + \cot\delta_\eta) \quad (44)$$

Equation (31) can be integrated from r = 1 to η to yield

$$- \rho_j q_j^2 (\eta^j \varepsilon_\eta \sin\delta_\eta \cos\delta_\eta - \varepsilon_1 \sin\delta_1 \cos\delta_1) + 2\beta \int_1^\eta r^j (p_j - p_w) dr = 0 \quad (45)$$

Consider the simplest approximation that

$$p_w \simeq [(\eta^2 - r^2) p_{w1} + (r^2 - 1) p_{w\eta}]/(\eta^2 - 1)$$

Equation (45) thus becomes

$$- \rho_j q_j^2 (\eta^j \varepsilon_\eta \sin\delta_\eta \cos\delta_\eta - \varepsilon_1 \sin\delta_1 \cos\delta_1) + 2\beta \left\{ p_j k_1 - \frac{[p_{w1}(\eta^2 k_1 - k_2) + p_{w\eta}(k_2 - k_1)]}{(\eta^2 - 1)} \right\} = 0 \quad (46)$$

where

$$k_1 = [\eta^{(j+1)} - 1]/(j + 1)$$

and

$$k_2 = [\eta^{(j+3)} - 1]/(j + 3)$$

Similarly, Equation (32) yields

$$\eta^j \varepsilon_\eta \left[q_j (1 - q_j^2)^{1/(\gamma-1)} \sin\delta_\eta + \left(\frac{\gamma - 1}{\gamma + 1}\right)^{1/2} \left(\frac{2}{\gamma + 1}\right)^{1/(\gamma-1)} \right]$$

$$= \varepsilon_1 \left[q_j (1 - q_j^2)^{1/(\gamma-1)} \sin\delta_1 + u_{w1} (1 - u_{w1}^2)^{1/(\gamma-1)} \right] \quad (47)$$

The basic governing nonlinear algebraic equations for the one-by-two formulation are Equations (39), (40) or (41), (46), (47) and (34) for the five basic unknowns: ε_0, ε_1, η, u_{w1} and δ_η. We note that it is the consideration of the surface sonic point which provides two conditions (Eqs. (33) and (34) at $r = \eta$) with one unknown (the location of η) that enables us to close the system. We shall designate solutions obtained from using Equation (40), the modified continuity equation, by the symbol MCE, and those from Equation (41), the global mass conservation equation, by the symbol GMC.

B. ONE-BY-THREE SOLUTION. In this formulation the wall-jet region is not modified. The shock layer is divided into two regions: $0 \le r \le \frac{1}{2}$ and $\frac{1}{2} \le r \le 1$. Denote the quantities evaluated at $r = \frac{1}{2}$ by the subscript 2 and consider a continuous approximating function

$$-\frac{d\varepsilon}{dr} = \cot\sigma \approx r[8(1-r^2)\cot\sigma_2 + (4r^2-1)\cot\sigma_1]/3 \tag{48}$$

Direct integration yields the equation of shock detachment distance

$$\varepsilon = \varepsilon_0 - r^2[(8\cot\sigma_2 - \cot\sigma_1) + 2(\cot\sigma_1 - 2\cot\sigma_2)r^2]/6$$

After some algebra, one may obtain the following relations between the shock angles and the detachment distances:

$$\cot\sigma_2 = (9\varepsilon_0 - \varepsilon_1 - 8\varepsilon_2)/3 \tag{49}$$

$$\cot\sigma_1 = (32\varepsilon_2 - 14\varepsilon_1 - 18\varepsilon_0)/3 \tag{50}$$

Equations (28) and (29) are of the form

$$\frac{df}{dr} + r^j g = 0 \tag{51}$$

where g is an even function of r. Therefore, one may obtain by straightforward integrations that

$$f_2 - f_0 + \int_0^{1/2} r^j g dr = 0 \tag{52}$$

and

$$f_1 - f_0 + \int_0^{1} r^j g dr = 0 \tag{53}$$

The even function g may be approximated by the Lagrangian interpolation formula

$$g \approx g_0(1-r^2)(1-4r^2) + g_1(4r^2-1)r^2/3 + 16g_2(1-r^2)r^2/3 \tag{54}$$

so that the integrals in Equations (52) and (53) become

$$\int_0^{1/2} r^j g dr \approx 2^{-(j+1)}(H_0 g_0 + H_1 g_1 + H_2 g_2) \tag{52a}$$

and

$$\int_0^{1} r^j g dr \approx I_0 g_0 + I_1 g_1 + I_2 g_2 \tag{53a}$$

where

$$H_0 = \frac{1}{(j+1)} - \frac{5}{4(j+3)} + \frac{1}{4(j+5)} \tag{52b}$$

$$H_1 = \frac{-1}{6(j+3)(j+5)} \tag{52c}$$

$$H_2 = \frac{(3j + 17)}{3(j + 3)(j + 5)} \tag{52d}$$

$$I_0 = \frac{1}{(j + 1)} - \frac{5}{(j + 3)} + \frac{4}{(j + 5)} \tag{53b}$$

$$I_1 = \frac{(3j + 7)}{3(j + 3)(j + 5)} \tag{53c}$$

and

$$I_2 = \frac{32}{(j + 3)(j + 5)} \tag{53d}$$

We therefore have four nonlinear algebraic equations obtainable from Equations (28) and (29). In addition, there are Equations (46), (47) and (34) of the wall-jet region. We now have two additional basic variables, namely, ε_2 and u_{w2}. The system is again closed. This formulation is termed the one-by-three MCE method. One may also consider a one-by-three GMC method by using Equation (41) to replace the equation obtained by integrating Equation (29) from r = 0 to 1.

It is obvious that other approximating functions can also be used. For example, if, instead of the continuous representation as given by Equation (54), the even function g is assumed to be only piecewise smooth such as

$$g \approx g_0 + 4r^2(g_2 - g_0) \quad \text{for} \quad 0 \le r \le \frac{1}{2}$$

and

$$g \approx \frac{1}{3}[4g_2 - g_1 + 4r^2(g_1 - g_2)] \quad \text{for} \quad \frac{1}{2} \le r \le 1$$

Equations (52) and (53) still hold but the constant coefficients, H's and I's, will be modified accordingly. This constitutes the one-by-three MCE-PWS method and the corresponding one-by-three GMC-PWS method. Of course Equations (48) to (50) will also be replaced by the following piecewise smooth equations:

For $0 \le r \le \frac{1}{2}$

$$\varepsilon = \varepsilon_0 - r^2 \cot\delta_2$$

and for $\frac{1}{2} \le r \le 1$

$$\varepsilon = \varepsilon_2 - \frac{(4r^2 - 1)}{48} [2(8 \cot\delta_2 - \cot\delta_1) + (4r^2 + 1)(\cot\delta_1 - 2 \cot\delta_2)]$$

where

$$\cot\delta_2 = 4(\varepsilon_0 - \varepsilon_2)$$

and

$$\cot\delta_1 = \frac{8}{3}(5\varepsilon_2 - 2\varepsilon_1 - 3\varepsilon_0)$$

Different approximating functions can also be used in the one-by-two method. One possible utilization is illustrated in the following consideration of the stagnation-point quantities.

C. <u>STAGNATION-POINT VELOCITY GRADIENT</u>. Of particular interest to us is the stagnation-point velocity gradient which is directly related to the heat-transfer rate. Since u_w is determined only at discrete locations in the scheme III of the method of integral relations, differentiation of an interpolation formula is not accurate. This difficulty can be circumvented by the following method.

Dividing Equation (28) by r^j and taking the limit as $r \to 0$, we obtain

$$(1 + j)\rho_{s0}v_{s0}\varepsilon_0\left(\frac{du_s}{dr}\right)_0 + 2\left\{\beta(p_{s0} - p_{w0}) + \rho_{s0}v_{s0}^2\right\} = 0$$

Similarly, Equation (29) yields

$$(1 + j)\varepsilon_0\left[(1 - v_{s0}^2)^{1/(\gamma-1)}\left(\frac{du_s}{dr}\right)_0 + \left(\frac{du_w}{dr}\right)_0\right] + 2v_{s0}(1 - v_{s0}^2)^{1/(\gamma-1)} = 0$$

Eliminating $(du_s/dr)_0$ from the above two equations, we obtain

$$\left(\frac{du_w}{dr}\right)_0 = \frac{2\beta(1 - v_{s0}^2)^{1/(\gamma-1)}(p_{s0} - p_{w0})}{(1 + j)\rho_{s0}v_{s0}\varepsilon_0} \tag{55}$$

At $r = 0$, $\sigma = \pi/2$. From Equations (23) to (26), (30) and (55), one may conclude that, for fixed values of M_∞ and γ, the stagnation-point velocity gradient is inversely proportional to the shock detachment distance at the stagnation point. Figure 2 shows the value of $(1 + j)\varepsilon_0\left(\frac{du_w}{dr}\right)_0$ as a function of M_∞ for $\gamma = 1.4$.

Since

$$\left(\frac{du_s}{dr}\right)_0 = \left(\frac{du_s}{d\sigma}\right)_0\left(\frac{d\sigma}{dr}\right)_0 = \frac{2(1 - M_\infty^2)V_\infty}{(\gamma + 1)M_\infty^2}\left(\frac{d\sigma}{dr}\right)_0$$

we may also obtain the relation that

$$\sigma_0' \equiv \left(\frac{d\sigma}{dr}\right)_0 = \frac{(\gamma + 1)M_\infty^2[\beta(p_{s0} - p_{w0}) + \rho_{s0}v_{s0}^2]}{(1 + j)(M_\infty^2 - 1)\rho_{s0}v_{s0}V_\infty\varepsilon_0} \tag{56}$$

Equation (56) may be used to generate slightly more complicated equations for the shock-layer thickness and the shock angle. For example, for the one-by-two method, we may replace Equation (35) by the following more complicated function

$$-\frac{d\varepsilon}{dr} = \cot\sigma \approx r[(r^2 - 1)\sigma_0' + r^2\cot\sigma_1] \tag{57}$$

Equations (36) and (37) are thus replaced by, respectively,

$$\varepsilon = \varepsilon_0 + r^2[\sigma_0'(2 - r^2) - r^2\cot\sigma_1]/4 \tag{58}$$

and

$$\cot\sigma_1 = \sigma_0' + 4(\varepsilon_0 - \varepsilon_1) \tag{59}$$

The forms of other equations are unmodified. This formulation is termed the one-by-two GMC (or MCE)-SP method. In essence, the utilization of Equation (56) has increased the order of the function by 2. For example, Equations (35) and (36) are, respectively, linear and quadratic in r, but Equations (57) and (58) are cubic and quartic in r, respectively. All one-by-three methods can be similarly modified by incorporating Equation (56) in their representation of the shock angle and the shock detachment distance, and will be termed accordingly.

RESULTS AND DISCUSSION

The governing coupled nonlinear algebraic equations are solved iteratively by the Newton-Raphson method. All of the one-strip solutions obtained so far are tabulated in Tables 1 to 3. Most of the results do not go above $M_\infty = 4$. This is because, for shock-interference problems, we are mostly interested in lower supersonic Mach numbers. There is, however, an upper limit on the free-stream Mach number above which no physically acceptable solutions can be obtained by the present one-strip formulation of the method of integral relations. This happens when the location of the surface sonic point, η, is along the line of the jet edge ($r = 1$). The trend, that η decreases toward unity as M_∞ increases as predicted by the theory, was also observed experimentally by Hunt and co-workers (Refs. (8) and (14)). However, the actual occurrence of $\eta = 1$ is believed to be due to the approximation introduced by the solution method. Fortunately, this generally occurs above $M_\infty = 4$ and hence is not of serious concern to us for the present problem.

(14) Carling, J. C. and Hunt, B. L., "The Near Wall Jet of a Normally Impinging, Uniform, Axisymmetric, Supersonic Jet," Journal of Fluid Mechanics, Vol. 66, 1974, pp. 159-176

There is also a lower limit on M_∞ below which no physically acceptable solutions can be obtained. For the planar case, this happens when the calculated value of M_{s1} reaches unity. The fact that it occurs at $M_\infty > 1$ is again due to the approximate nature of the solution method. For the axisymmetric case, this happens at a much higher value of M_∞, and the reason for its occurrence is not understood at the present time. Fortunately, a quite wide range of M_∞ does exist between which meaningful solutions have been obtained. Because of this much higher value of the lower limit on M_∞ for the axisymmetric case, the majority of the results obtained is for the planar case and these results will be discussed first. The results for axisymmetric flows will be briefly considered later. All results shown are for $\gamma = 1.4$.

PLANAR JET IMPINGEMENT

The results of the stagnation-point velocity gradient as obtained by the various methods are shown in Figures 3 and 4 as a function of M_∞. All solutions show the same trend, namely, the initial rapid increase of $\left(\frac{du_w}{dr}\right)_0$ at low Mach numbers, and the slow rise toward the asymptote at high Mach numbers. The difference between one-by-two and one-by-three formulations is seen to be moderate at high Mach numbers, and it drops very rapidly as M_∞ is decreased. The same can be said in regard to the different choice of the governing equations between GMC and MCE methods. The application of more complicated profiles (SP method) greatly reduces the differences between one-by-two and one-by-three formulations, but one-by-three results display only small effects by the application of these more complicated profiles. In fact, results indicate that the one-by-three formulation is quite insensitive to different approximating functions employed in general. This is not always the case when other quantities away from the stagnation point are considered, as we shall see later.

The detachment distance of the shock and the upper boundary of the wall jet as predicted by the corresponding one-by-two and one-by-three formulations is shown in Figures 5 to 7 according to different applications of the method of integral relations. All results show the following trend: (1) both the shock layer and the wall-jet layer become thicker as M_∞ decreases; (2) as M_∞ decreases, the location of the surface sonic point moves away from the line of the jet edge ($r = 1$); and (3) for a fixed M_∞, the moderate difference between one-by-two and one-by-three formulations at the symmetry line ($r = 0$) is reduced even further at the line of the jet edge ($r = 1$).

The surface Mach number evaluated at $r = 1$, M_{w1}, and the Mach number behind the shock at $r = 1$, M_{s1}, are depicted in Figure 8 as functions of M_∞. Clearly, neither M_{w1} nor M_{s1} is generally equal to unity. Hence the boundary conditions employed in References (8) and (9) are incorrect. The corresponding values of the shock angle at the line of the jet edge, σ_1, as obtained from various methods are shown in Figures 9 and 10. Similar to M_{s1}, they are seen to be more method-dependent than quantities such as M_{w1}.

The surface pressure distribution, as shown in Figure 11, indicates the general insensitivity of the results to various schemes employed. The only noticeable difference is the somewhat fuller profile predicted by the one-by-three formulation.

It therefore appears from self-consistency that reasonable engineering solutions for the stagnation-point velocity gradient (hence ϵ_0) and M_{w1} (hence u_{w1} and p_{w1}) have been obtained. Since heat-transfer rate is proportional to the square root of the velocity gradient at the stagnation point (Refs. (15) and (16)), peak-heating prediction is thus even less method-dependent. This, however, is in direct contrast to the axisymmetric case which, to be discussed next, is seen to be far from converging.

AXISYMMETRIC JET IMPINGEMENT

Among all the methods employed, only one-by-two GMC and MCE schemes have produced solutions which appear not to violate some of the obvious physical constraints such as $p_{w0} > p_{w2} > p_{w1} > p_{w\eta}$ and, as M_∞ decreases, both $(du_w/dr)_0$ and u_{w1} will also decrease. The results are tabulated in Tables 3a and 3b. The lowest M_∞ shown in each table is the lower limit of the Mach number below which no solution is obtainable. As we can see, the corresponding M_{s1} is far from being unity. The reason for the existence of this relatively high value of the lower limit of M_∞ is not understood at the present time.

The axisymmetric results are qualitatively similar to the planar solutions. There are noticeable differences also. For example, for the axisymmetric case, the shock-layer thickness drops off at a much faster rate as one moves away from the stagnation point. This results in a smaller shock angle, σ_1, and a thinner wall-jet layer. In fact, the rate that σ_1 drops with respect to decreasing M_∞ is so large that M_{s1} turns out to be increasing slightly as M_∞ is decreased. This trend is clearly opposite to that of the planar case which shows the

(15) Cohen, C. B. and Reshotko, E., "Similar Solutions for the Compressible Laminar Boundary Layer with Heat Transfer and Pressure Gradient," NACA Rpt 1293, Lewis Research Center, Cleveland, Ohio, 1956

(16) Fay, J. A. and Riddell, F. R., "Theory of Stagnation Point Heat Transfer in Dissociated Air," Journal of the Aeronautical Sciences, Vol. 25, 1958, pp. 73-85, 121

monotonic decreasing behavior as was depicted in Figure 8. Since the axisymmetric solution appears to be very method-dependent (as can be seen easily by the fact that even one-by-two GMC- and MCE-SP methods yield no physically acceptable solutions), results obtained by other methods are needed before these different trends can be ascertained or refuted.

CONCLUSIONS

The major conclusion that we may draw from the present study is that solutions that satisfy all well-posed boundary conditions can be obtained by the one-strip formulation of the method of integral relations. The application of the scheme III of the method has enabled us to avoid both the unwanted singularity at the low supersonic Mach number and the numerical difficulty of satisfying the regularity condition at the surface sonic point peculiar to the scheme I of the method. Rational engineering solutions for the stagnation-point velocity gradient and, hence, the peak heat-transfer rate have been obtained for a planar supersonic balanced jet impinging normally on a flat surface. However, more theoretical and/or experimental studies are needed before present results can be quantitatively assessed. Toward this goal, a two-strip formulation of the method of integral relations has been completed. Unfortunately, because of the time limitations, no quantitative results have yet been obtained. For the sake of completeness, this formulation is included in the Appendix.

Since, for impingement angles between normal (90 degrees) and about 50 degrees, the effect of the angle of impingement on the peak pressure was found experimentally by Henderson (Ref. (17)) to be small, the present planar jet-impingement model might be coupled with the shock-interference model of Edney (Ref. (1)) as programmed by Morris and Keyes (Ref. (18)) to predict type IV shock-interaction effects. In view of the extremely short computer time required by the present method (typically less than five seconds on a CDC 6500 computer for one converged solution at one Mach number), this approach is indeed very attractive.

(17) Henderson, L. F., "Experiments on the Impingement of a Supersonic Jet on a Flat Plate," ZAMP, Vol. 17, 1966, pp. 553-569

(18) Morris, D. J. and Keyes, J. W., "Computer Programs for Predicting Supersonic and Hypersonic Interference Flow Fields and Heating," NASA TM X-2725, Langley Research Center, Hampton, Va. 1973

Table 1 PLANAR JET IMPINGEMENT: ONE-BY-TWO SOLUTIONS
a. GMC Method

M_∞	$\left(\frac{du_w}{dr}\right)_0$	ε_0	ε_1	ε_n	η	p_{w0}	p_{w1}	p_{wn}	σ_1	δ_1	δ_n	M_j	M_{s1}
5.0	0.1843	0.9499	0.6202	0.6196	1.019	0.0617	0.0338	0.0326	0.9878	1.505	1.571	3.371	1.392
4.5	0.1825	0.9765	0.6472	0.6448	1.040	0.0917	0.0519	0.0484	0.9884	1.452	1.571	3.199	1.364
4.0	0.1799	1.014	0.6354	0.6784	1.072	0.1388	0.0819	0.0733	0.9895	1.387	1.571	3.006	1.328
3.5	0.1761	1.069	0.7423	0.7245	1.123	0.2130	0.1330	0.1125	0.9918	1.303	1.571	2.787	1.281
3.0	0.1701	1.157	0.8341	0.7888	1.206	0.3283	0.2213	0.1735	0.9969	1.191	1.571	2.535	1.221
2.5	0.1594	1.317	1.002	0.8803	1.347	0.4990	0.3722	0.2636	1.009	1.031	1.571	2.241	1.144
2.25	0.1505	1.457	1.150	0.9399	1.452	0.6055	0.4803	0.3199	1.020	0.9231	1.571	2.074	1.099
2.0	0.1368	1.689	1.392	1.010	1.592	0.7209	0.6113	0.3808	1.036	0.7873	1.571	1.893	1.053
1.9	0.1295	1.829	1.539	1.042	1.660	0.7674	0.6687	0.4054	1.045	0.7233	1.571	1.816	1.036
1.8	0.1206	2.016	1.732	1.075	1.735	0.8127	0.7275	0.4293	1.054	0.6529	1.571	1.737	1.020
1.7	0.1100	2.276	1.999	1.109	1.819	0.8557	0.7860	0.4521	1.065	0.5759	1.571	1.655	1.008
1.64	0.1026	2.484	2.211	1.131	1.874	0.8799	0.8201	0.4649	1.072	0.5265	1.571	1.604	1.002

Table 1 (Cont'd)

b. MCE Method

M_∞	$\left(\frac{du_w}{dr}\right)_0$	ϵ_0	ϵ_1	ϵ_η	η	p_{w0}	p_{w1}	$p_{w\eta}$	σ_1	δ_1	δ_η	M_j	M_{s1}
4.0	0.1738	1.049	0.7424	0.7374	1.064	0.1388	0.0803	0.0733	1.020	1.420	1.571	2.967	1.256
3.5	0.1715	1.098	0.7887	0.7732	1.118	0.2130	0.1310	0.1125	1.017	1.328	1.571	2.761	1.227
3.0	0.1671	1.178	0.8677	0.8245	1.206	0.3283	0.2192	0.1735	1.015	1.207	1.571	2.520	1.185
2.5	0.1580	1.329	1.022	0.9010	1.349	0.4990	0.3708	0.2636	1.020	1.039	1.571	2.234	1.124
2.25	0.1496	1.465	1.163	0.9532	1.455	0.6055	0.4794	0.3199	1.027	0.9276	1.571	2.071	1.087
2.0	0.1365	1.693	1.400	1.017	1.594	0.7209	0.6110	0.3808	1.041	0.7894	1.571	1.891	1.046
1.9	0.1292	1.832	1.544	1.047	1.662	0.7674	0.6685	0.4054	1.048	0.7247	1.571	1.815	1.031
1.8	0.1204	2.019	1.736	1.078	1.737	0.8127	0.7274	0.4293	1.057	0.6538	1.571	1.736	1.017
1.7	0.1099	2.277	2.002	1.112	1.820	0.8557	0.7860	0.4521	1.067	0.5763	1.571	1.654	1.006
1.64	0.1026	2.485	2.213	1.132	1.875	0.8799	0.8201	0.4649	1.073	0.5268	1.571	1.604	1.000

c. GMC-SP Method

M_∞	$\left(\frac{du_w}{dr}\right)_0$	ϵ_0	ϵ_1	ϵ_η	η	p_{w0}	p_{w1}	$p_{w\eta}$	σ_1	δ_1	δ_η	M_j	M_{s1}
4.0	0.1978	0.9219	0.6854	0.6784	1.072	0.1388	0.0819	0.0733	0.9895	1.387	1.571	3.006	1.328
3.5	0.1922	0.9799	0.7423	0.7245	1.123	0.2130	0.1330	0.1125	0.9918	1.303	1.571	2.787	1.281
3.0	0.1836	1.073	0.8341	0.7888	1.206	0.3283	0.2213	0.1735	0.9969	1.191	1.571	2.535	1.221
2.5	0.1693	1.240	1.002	0.8803	1.347	0.4990	0.3722	0.2636	1.009	1.031	1.571	2.241	1.144
2.25	0.1582	1.386	1.150	0.9399	1.452	0.6055	0.4803	0.3199	1.020	0.9231	1.571	2.074	1.099
2.0	0.1422	1.625	1.392	1.010	1.592	0.7209	0.6113	0.3808	1.036	0.7873	1.571	1.893	1.053
1.9	0.1339	1.769	1.539	1.042	1.660	0.7674	0.6687	0.4054	1.045	0.7233	1.571	1.816	1.036
1.8	0.1241	1.959	1.732	1.075	1.735	0.8127	0.7275	0.4293	1.054	0.6529	1.571	1.737	1.020
1.75	0.1186	2.079	1.854	1.092	1.776	0.8346	0.7569	0.4409	1.059	0.6152	1.571	1.696	1.014

Table 2 PLANAR JET IMPINGEMENT: ONE-BY-THREE SOLUTIONS

a. GMC Method

M_∞	$\left(\frac{du_w}{dr}\right)_0$	ϵ_0	ϵ_1	ϵ_n	n	p_{w0}	p_{w1}	p_{wn}	σ_1	δ_1	δ_n	M_j	M_{s1}
4.7	0.2081	0.8498	0.65580	0.65579	1.001	0.0781	0.04134	0.04125	1.077	1.567	1.571	3.147	1.161
4.5	0.2069	0.8612	0.6663	0.6662	1.010	0.0917	0.0493	0.0484	1.076	1.541	1.571	3.082	1.155
4.0	0.2032	0.8978	0.7005	0.6982	1.041	0.1388	0.0780	0.0733	1.073	1.466	1.571	2.906	1.138
3.5	0.1977	0.9526	0.7519	0.7421	1.093	0.2130	0.1275	0.1125	1.070	1.370	1.571	2.708	1.115
3.0	0.1890	1.041	0.8365	0.8033	1.179	0.3283	0.2141	0.1735	1.067	1.242	1.571	2.479	1.085
2.5	0.1741	1.206	0.9960	0.8901	1.327	0.4990	0.3650	0.2636	1.066	1.063	1.571	2.208	1.046
2.25	0.1622	1.351	1.139	0.9466	1.438	0.6055	0.4744	0.3199	1.067	0.9447	1.571	2.053	1.023
2.0	0.1452	1.592	1.380	1.013	1.582	0.7209	0.6076	0.3308	1.073	0.7984	1.571	1.881	1.001

b. MCE Method

M_∞	$\left(\frac{du_w}{dr}\right)_0$	ϵ_0	ϵ_1	ϵ_n	n	p_{w0}	p_{w1}	p_{wn}	σ_1	δ_1	δ_n	M_j	M_{s1}
4.0	0.1917	0.9515	0.7698	0.7682	1.036	0.1388	0.0770	0.0733	1.112	1.486	1.571	2.866	1.055
3.5	0.1884	0.9993	0.8121	0.8032	1.091	0.2130	0.1261	0.1125	1.104	1.385	1.571	2.677	1.047
3.0	0.1824	1.079	0.8850	0.8522	1.182	0.3283	0.2125	0.1735	1.094	1.252	1.571	2.458	1.034
2.5	0.1703	1.233	1.030	0.9231	1.334	0.4990	0.3638	0.2636	1.085	1.068	1.571	2.197	1.014
2.35	0.1645	1.309	1.104	0.9505	1.397	0.5615	0.4268	0.2966	1.083	0.9983	1.571	2.108	1.006

c. GMC-PWS Method

M_∞	$\left(\frac{du_w}{dr}\right)_0$	ϵ_0	ϵ_1	ϵ_n	n	p_{w0}	p_{w1}	p_{wn}	σ_1	δ_1	δ_n	M_j	M_{s1}
4.0	0.2017	0.9042	0.6924	0.6889	1.052	0.1388	0.0793	0.0733	1.040	1.439	1.571	2.944	1.211
3.5	0.1961	0.9602	0.7460	0.7338	1.103	0.2130	0.1293	0.1125	1.039	1.348	1.571	2.738	1.179
3.0	0.1874	1.051	0.8335	0.7965	1.188	0.3283	0.2165	0.1735	1.039	1.226	1.571	2.500	1.138
2.5	0.1726	1.216	0.9964	0.8857	1.333	0.4990	0.3674	0.2636	1.043	1.053	1.571	2.221	1.084
2.25	0.1609	1.362	1.142	0.9437	1.442	0.6055	0.4764	0.3199	1.049	0.9385	1.571	2.061	1.052
2.0	0.1442	1.602	1.383	1.012	1.585	0.7209	0.6088	0.3808	1.059	0.7958	1.571	1.886	1.021
1.9	0.1356	1.747	1.529	1.043	1.654	0.7674	0.6668	0.4054	1.064	0.7293	1.571	1.811	1.009

Table 2 (Cont'd)

d. GMC-SP Method

M_∞	$\left(\frac{du_w}{dr}\right)_0$	ε_o	ε_1	ε_n	η	p_{w0}	p_{w1}	p_{wn}	σ_1	δ_1	δ_n	M_j	M_{s1}
4.0	0.2039	0.8946	0.7002	0.6980	1.041	0.1388	0.0781	0.0733	1.073	1.465	1.571	2.907	1.140
3.5	0.1983	0.9494	0.7517	0.7418	1.093	0.2130	0.1275	0.1125	1.069	1.369	1.571	2.709	1.117
3.0	0.1896	1.038	0.8364	0.8031	1.179	0.3283	0.2141	0.1735	1.066	1.242	1.571	2.479	1.086
2.5	0.1746	1.203	0.9960	0.8900	1.327	0.4990	0.3651	0.2636	1.065	1.063	1.571	2.206	1.047
2.25	0.1626	1.348	1.139	0.9465	1.438	0.6055	0.4745	0.3199	1.067	0.9446	1.571	2.053	1.024
2.20	0.1596	1.387	1.177	0.9590	1.464	0.6281	0.4993	0.3318	1.068	0.9178	1.571	2.020	1.019

e. GMC-PWS-SP Method

M_∞	$\left(\frac{du_w}{dr}\right)_0$	ε_o	ε_1	ε_n	η	p_{w0}	p_{w1}	p_{wn}	σ_1	δ_1	δ_n	M_j	M_{s1}
4.0	0.2021	0.9023	0.6924	0.6889	1.052	0.1388	0.0793	0.0733	1.040	1.439	1.571	2.944	1.211
3.5	0.1965	0.9584	0.7460	0.7338	1.103	0.2130	0.1293	0.1125	1.039	1.348	1.571	2.738	1.179
3.0	0.1877	1.049	0.8335	0.7965	1.188	0.3283	0.2165	0.1735	1.039	1.226	1.571	2.500	1.138
2.5	0.1729	1.215	0.9964	0.8857	1.333	0.4990	0.3674	0.2636	1.043	1.053	1.571	2.221	1.084
2.25	0.1611	1.360	1.142	0.9437	1.442	0.6055	0.4764	0.3199	1.049	0.9385	1.571	2.061	1.052
2.0	0.1444	1.601	1.383	1.012	1.585	0.7209	0.6088	0.3808	1.059	0.7958	1.571	1.886	1.021
1.9	0.1357	1.745	1.529	1.043	1.654	0.7674	0.6668	0.4054	1.064	0.7293	1.571	1.811	1.009

f. MCE-PWS-SP Method

M_∞	$\left(\frac{du_w}{dr}\right)_0$	ε_o	ε_1	ε_n	η	p_{w0}	p_{w1}	p_{wn}	σ_1	δ_1	δ_n	M_j	M_{s1}
4.0	0.1912	0.9542	0.7597	0.7574	1.043	0.1388	0.0779	0.0733	1.077	1.468	1.571	2.902	1.129
3.5	0.1878	1.003	0.8033	0.7928	1.099	0.2130	0.1274	0.1125	1.071	1.370	1.571	2.707	1.113
3.0	0.1817	1.083	0.8782	0.8428	1.189	0.3283	0.2144	0.1735	1.064	1.241	1.571	2.481	1.090
2.5	0.1696	1.238	1.026	0.9159	1.338	0.4990	0.3658	0.2636	1.060	1.061	1.571	2.211	1.055
2.25	0.1591	1.378	1.164	0.9651	1.448	0.6055	0.4753	0.3199	1.062	0.9432	1.571	2.055	1.032
2.0	0.1433	1.613	1.398	1.025	1.590	0.7209	0.6083	0.3808	1.068	0.7978	1.571	1.883	1.008

Table 3 AXISYMMETRIC JET IMPINGEMENT: ONE-BY-TWO SOLUTIONS

a. GMC Method

M_∞	$\left(\frac{du_w}{dr}\right)_0$	ε_0	ε_1	ε_n	η	p_{w0}	p_{w1}	p_{wn}	σ_1	δ_1	δ_n	M_j	M_{s1}
4.5	0.1052	0.8466	0.3325	0.3297	1.006	0.0917	0.0494	0.0484	0.7715	1.127	1.168	3.572	1.969
4.0	0.09998	0.9122	0.3631	0.3521	1.020	0.1388	0.0777	0.0733	0.7386	1.017	1.144	3.385	1.998
3.75	0.09390	0.9855	0.3910	0.3701	1.034	0.1717	0.0992	0.0907	0.6992	0.9167	1.131	3.307	2.070
3.70	0.09138	1.016	0.4008	0.3760	1.038	0.1792	0.1047	0.0947	0.6824	0.8804	1.129	3.302	2.110
3.67	0.08853	1.051	0.4108	0.3820	1.042	0.1839	0.1085	0.0971	0.6632	0.8424	1.127	3.312	2.161

b. MCE Method

M_∞	$\left(\frac{du_w}{dr}\right)_0$	ε_0	ε_1	ε_n	η	p_{w0}	p_{w1}	p_{wn}	σ_1	δ_1	δ_n	M_j	M_{s1}
4.5	0.1051	0.8479	0.3311	0.3277	1.007	0.0917	0.0496	0.0484	0.7689	1.123	1.172	3.577	1.977
4.0	0.09766	0.9338	0.3531	0.3353	1.032	0.1388	0.0811	0.0733	0.7108	0.9696	1.179	3.433	2.083
3.9	0.09382	0.9774	0.3614	0.3366	1.042	0.1510	0.0911	0.0798	0.6818	0.9067	1.186	3.425	2.155
3.87	0.09141	1.005	0.3656	0.3367	1.046	0.1549	0.0951	0.0818	0.6637	0.8708	1.191	3.437	2.206

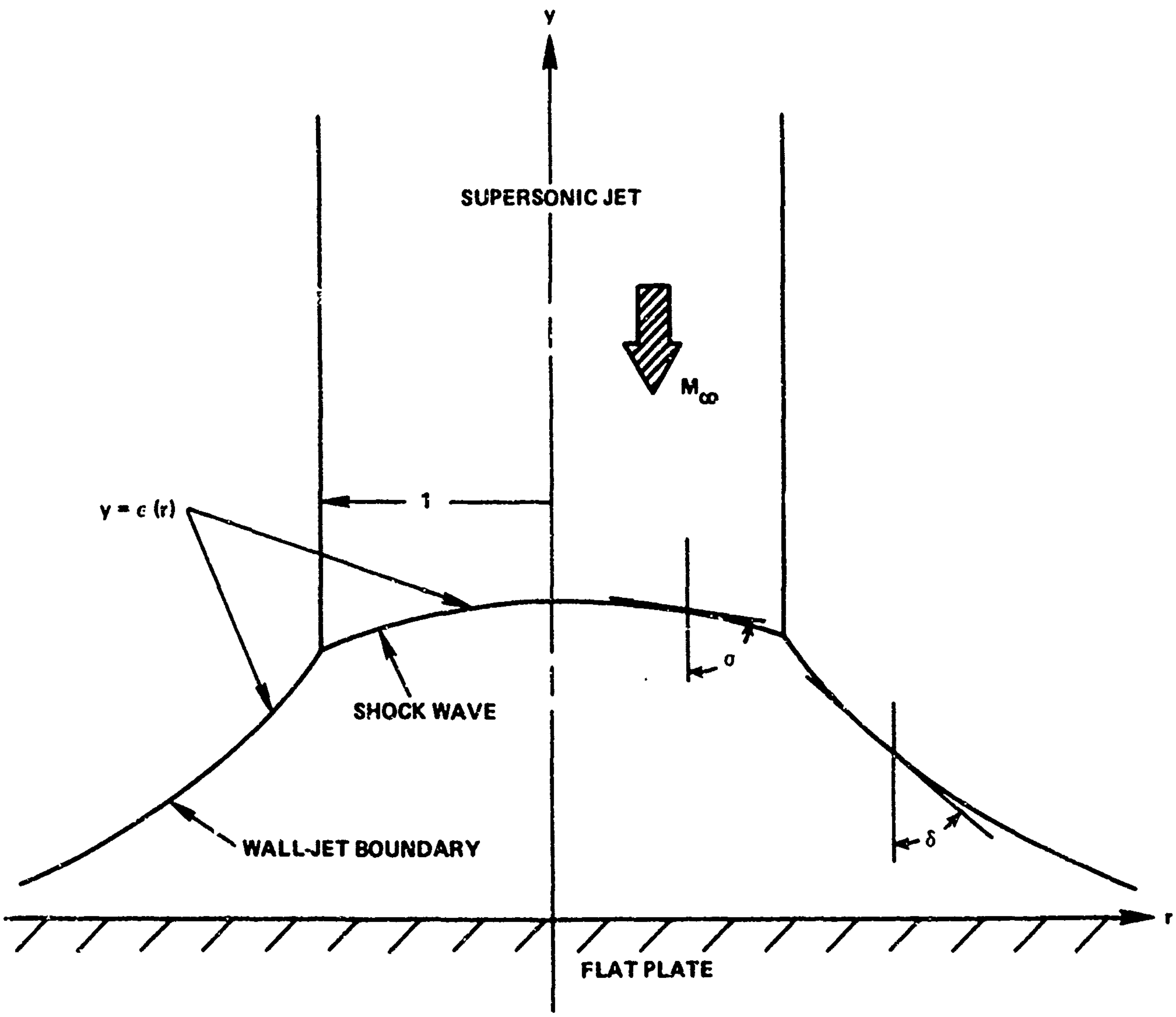

FIG. 1 SCHEMATIC DIAGRAM

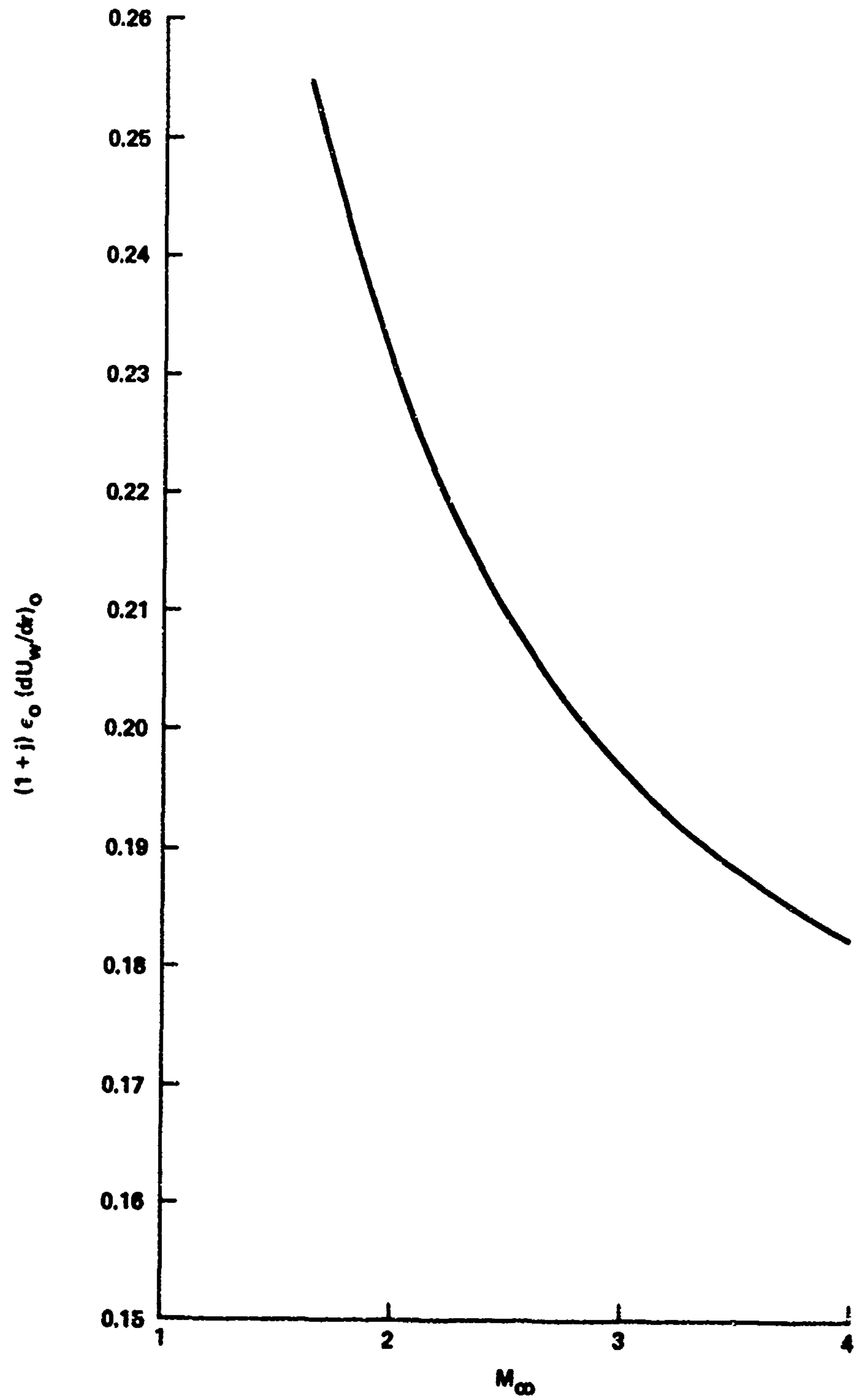

FIG. 2 UNIVERSAL CURVE FOR $\gamma = 1.4$

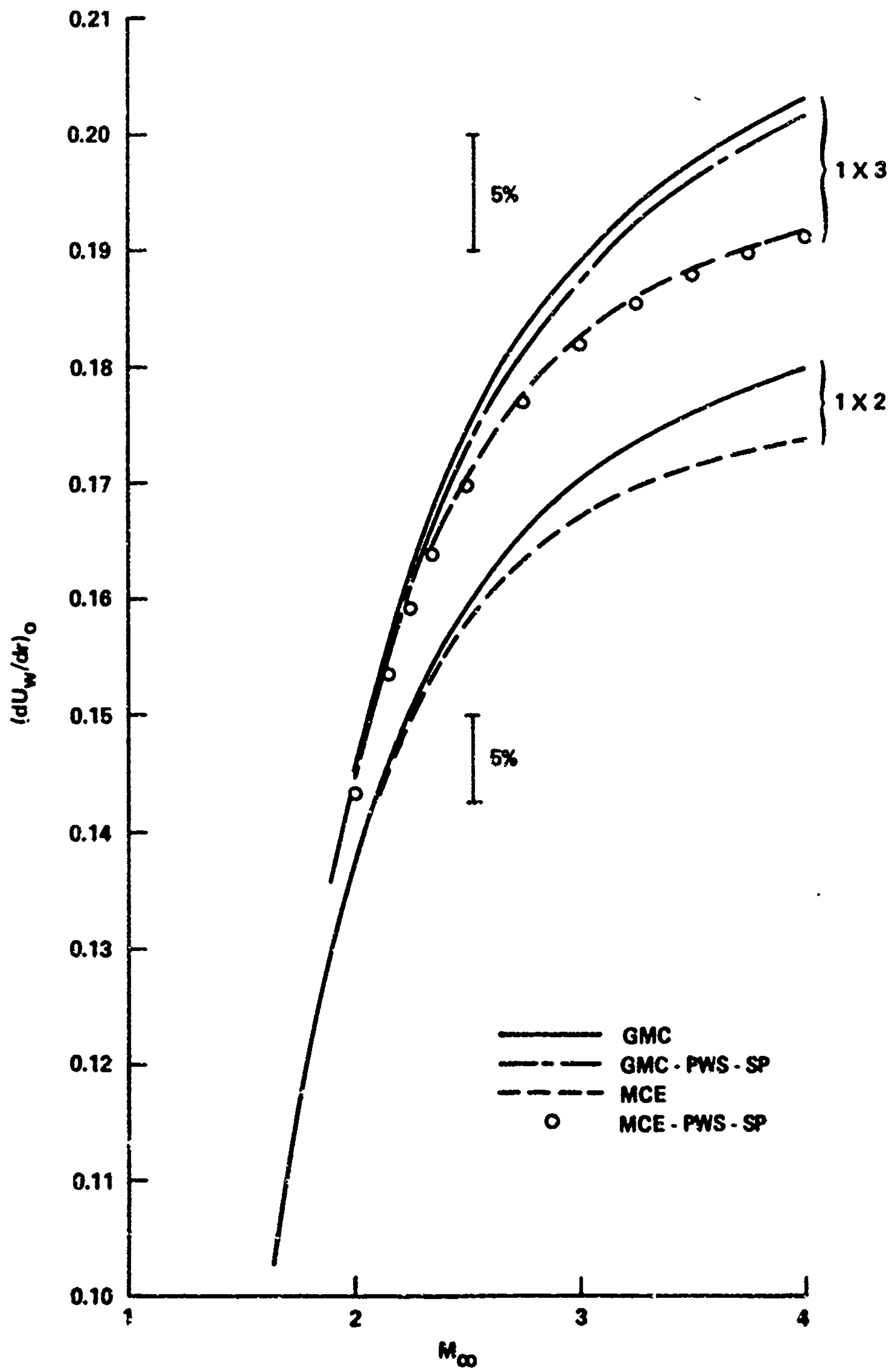

FIG. 3 STAGNATION-POINT VELOCITY GRADIENT: COMPARISON BETWEEN GMC AND MCE METHODS FOR PLANAR CASE

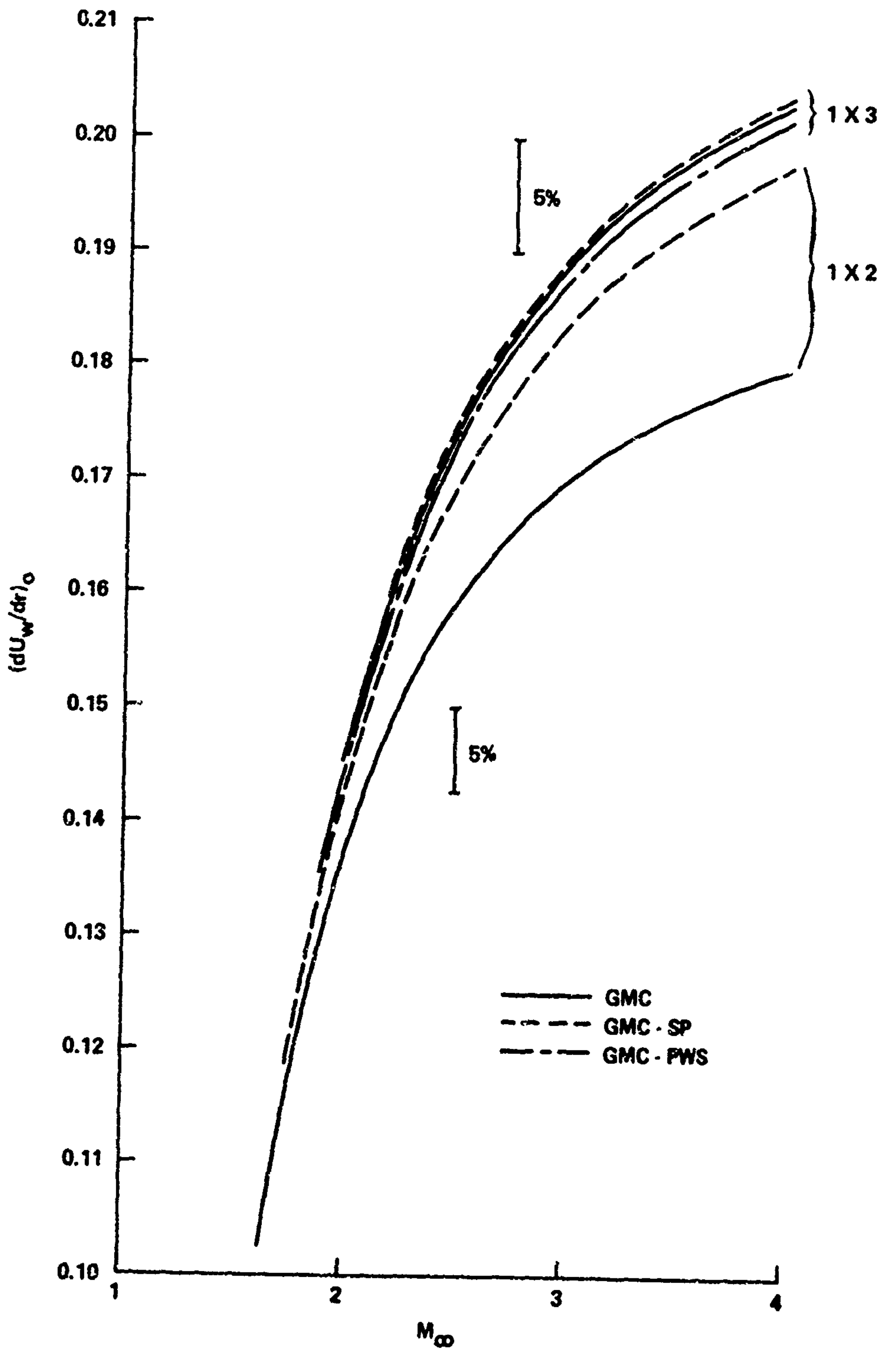

FIG. 4 STAGNATION-POINT VELOCITY GRADIENT: EFFECTS OF APPROXIMATING FUNCTIONS FOR PLANAR CASE

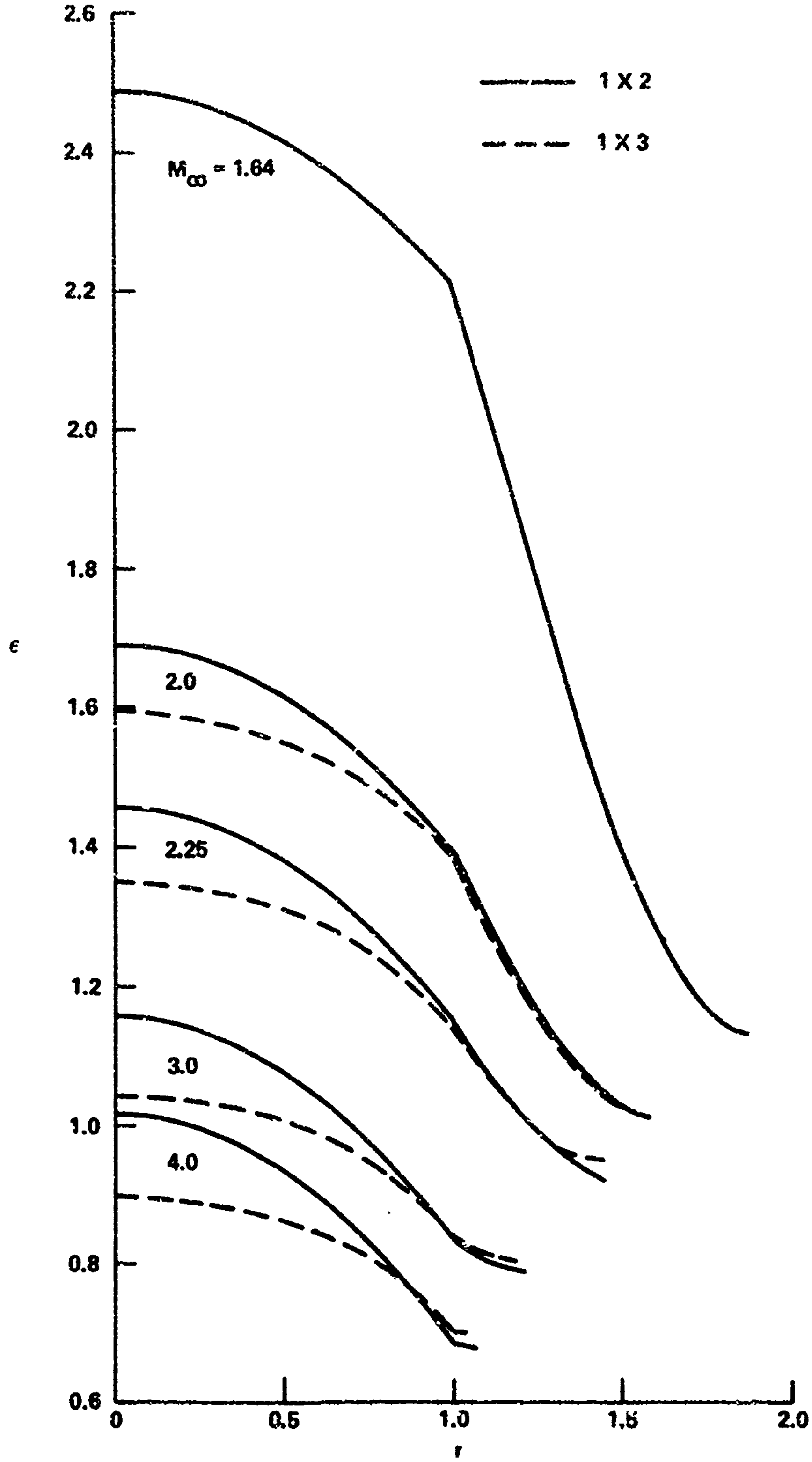

FIG. 5 THICKNESS DISTRIBUTION: GMC METHODS FOR PLANAR CASE

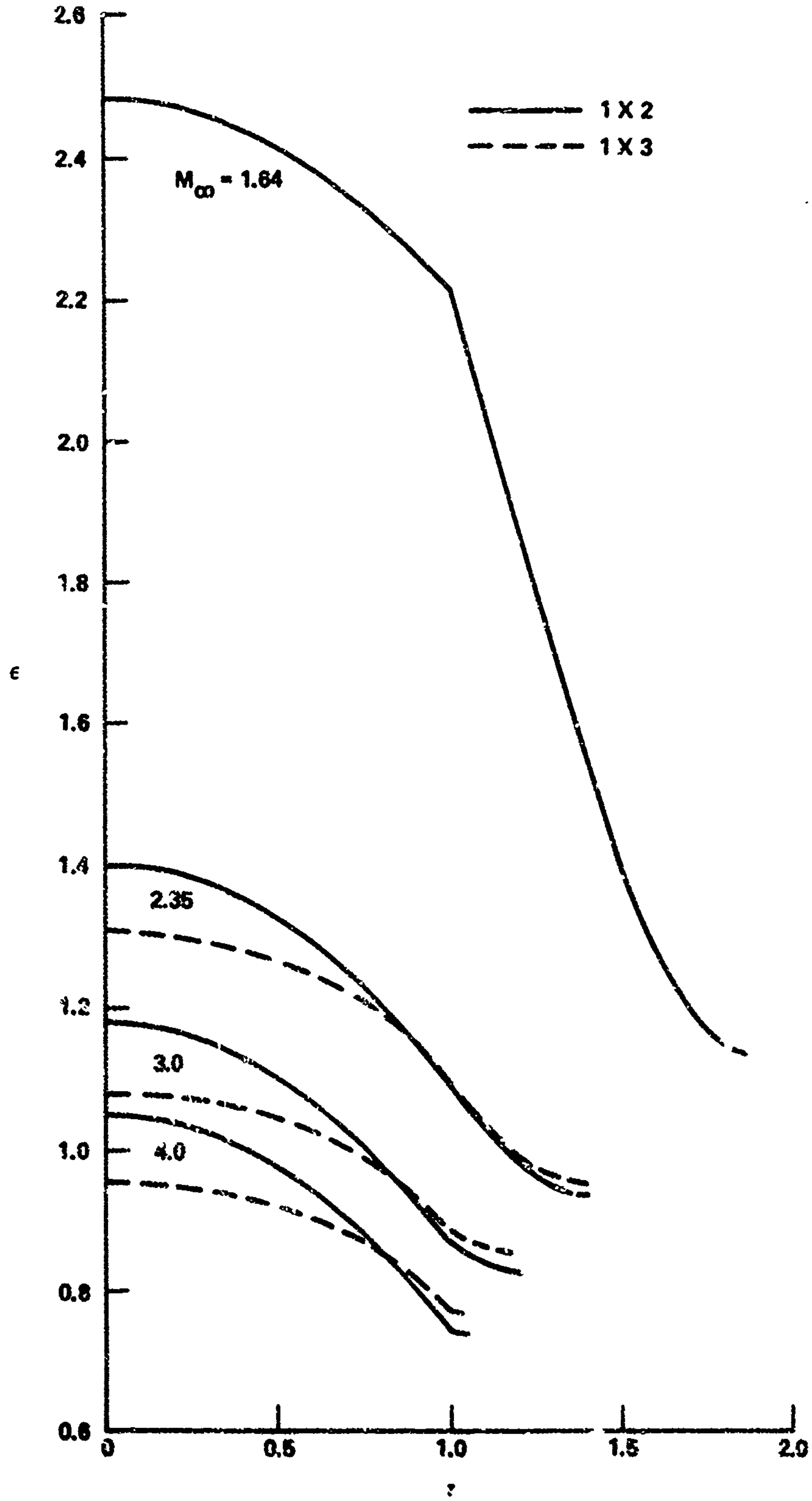

FIG. 6 THICKNESS DISTRIBUTION: MCE METHODS FOR PLANAR CASE

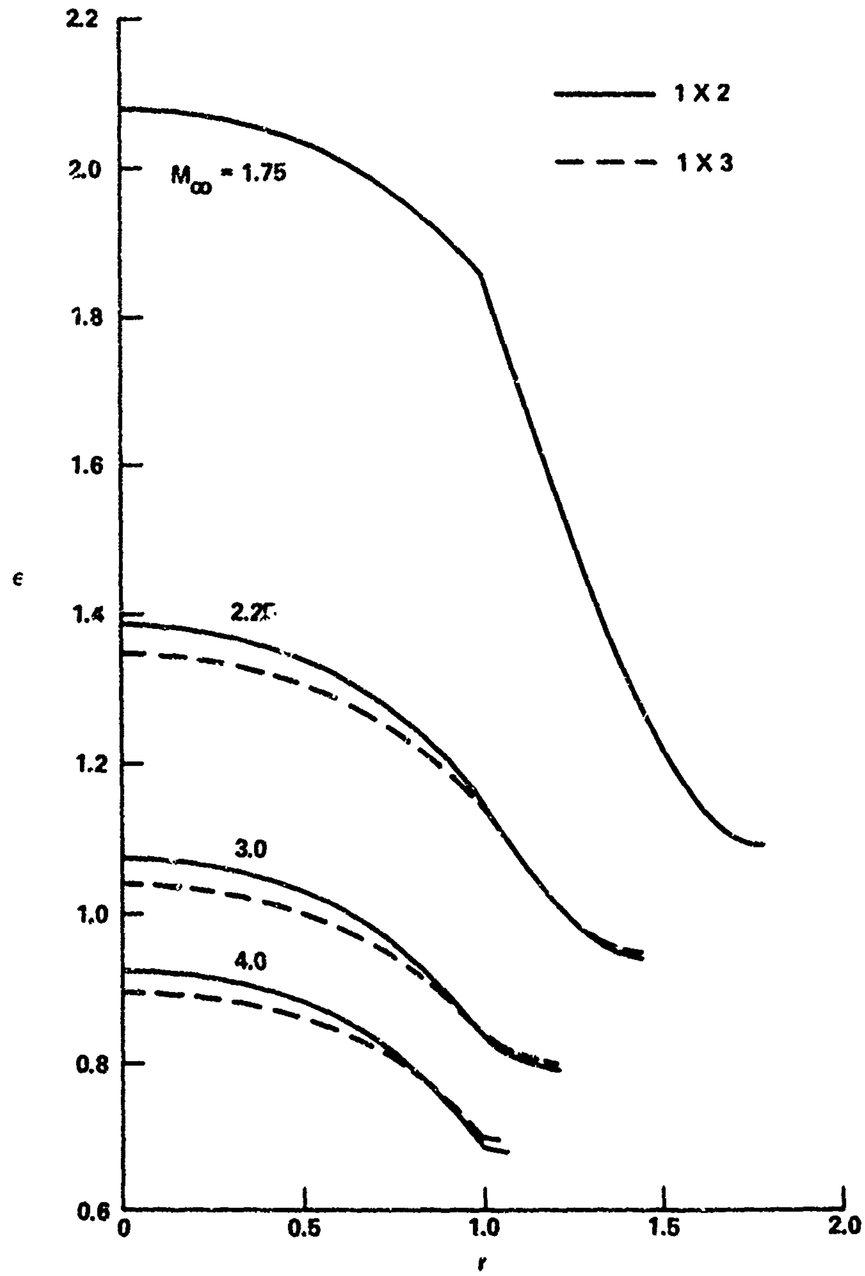

FIG. 7 THICKNESS DISTRIBUTION: GMC - SP METHODS FOR PLANAR CASE

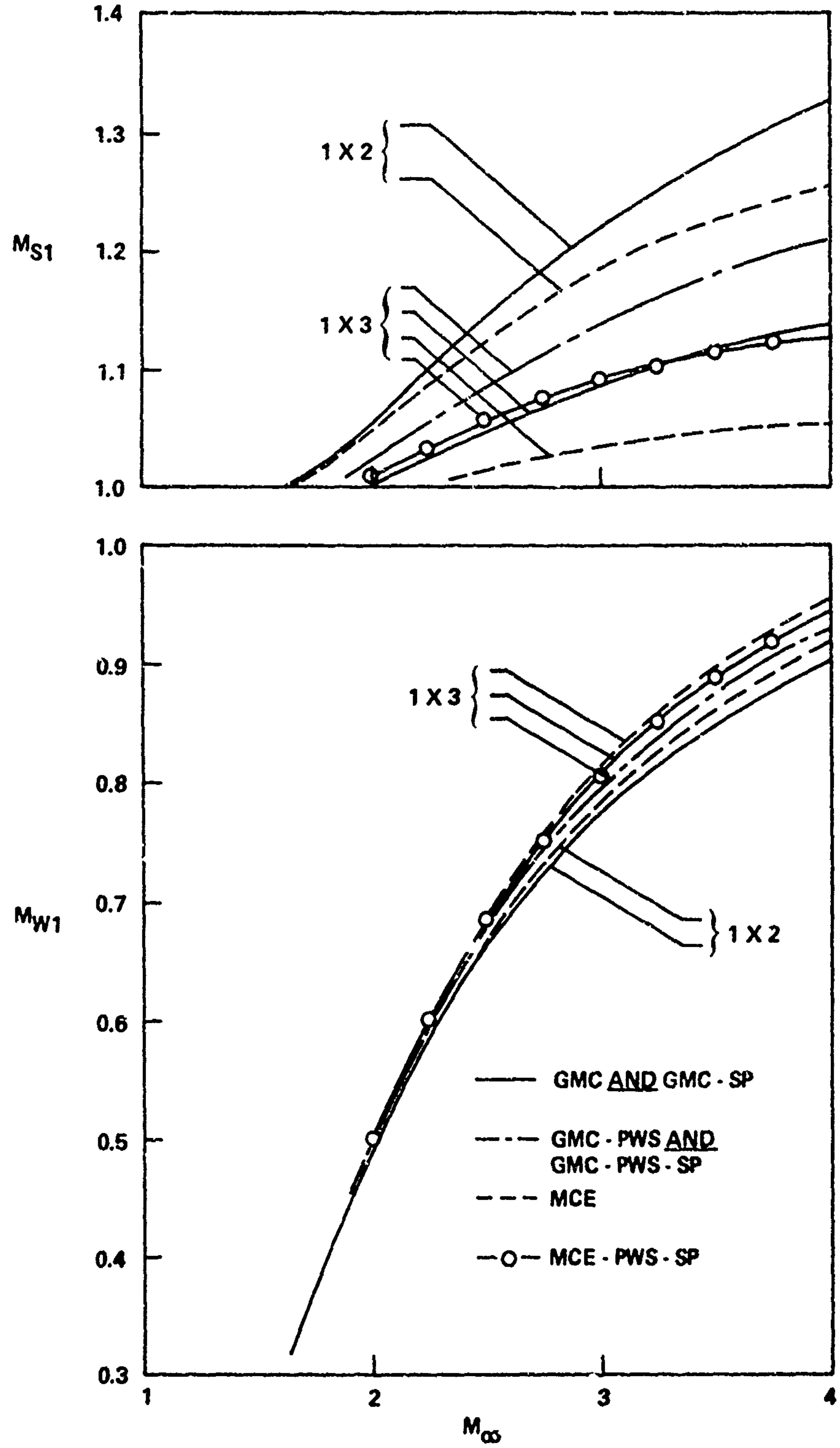

FIG. 8 MACH NUMBER BEHIND SHOCK AND PLATE MACH NUMBER AT r = 1 FOR PLANAR CASE

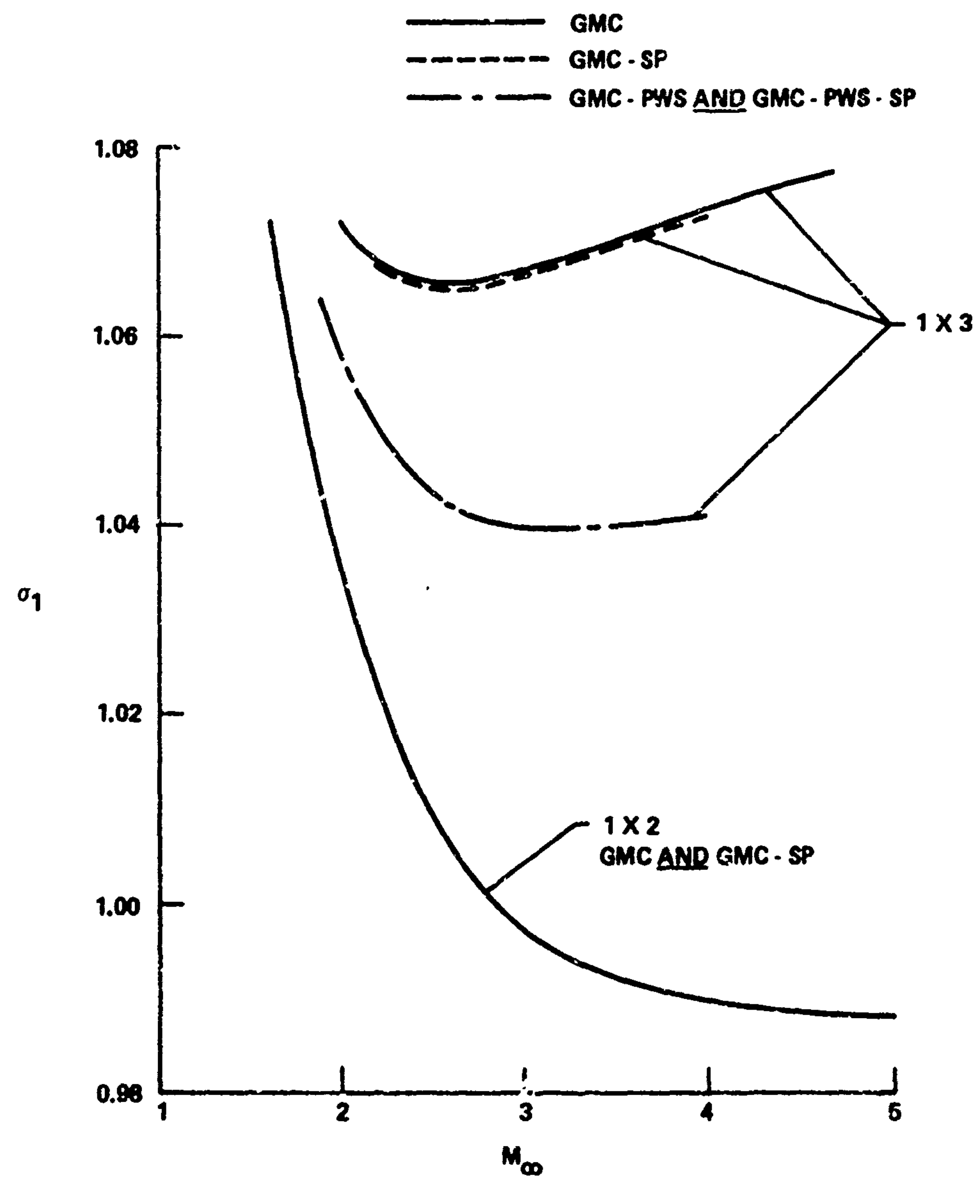

FIG. 9 SHOCK ANGLE AT r = 1: EFFECTS OF APPROXIMATING FUNCTIONS FOR PLANAR CASE

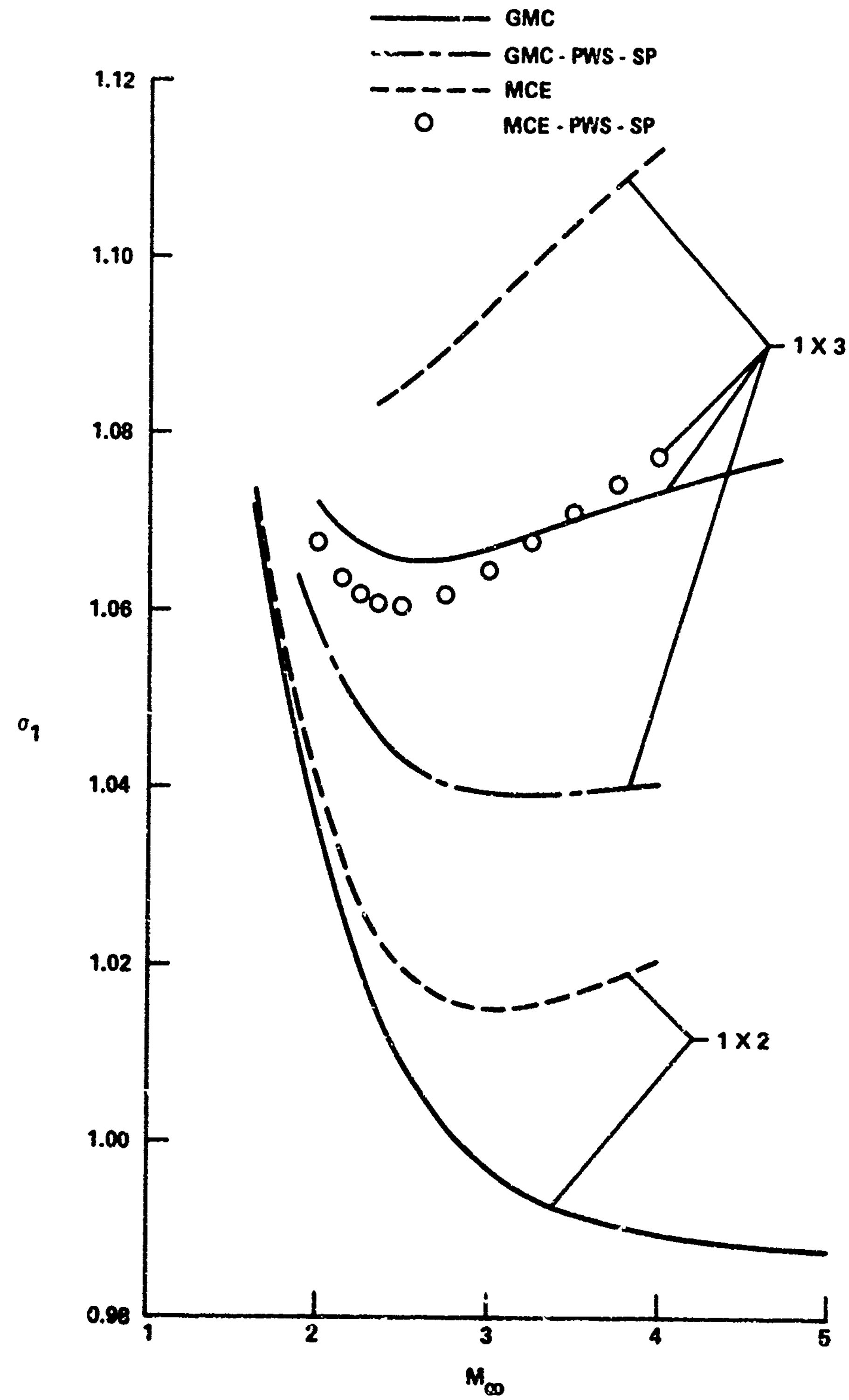

FIG. ^. SHOCK ANGLE AT r = 1: COMPARISON BETWEEN GMC AND MCE METHODS FOR PLANAR CASE

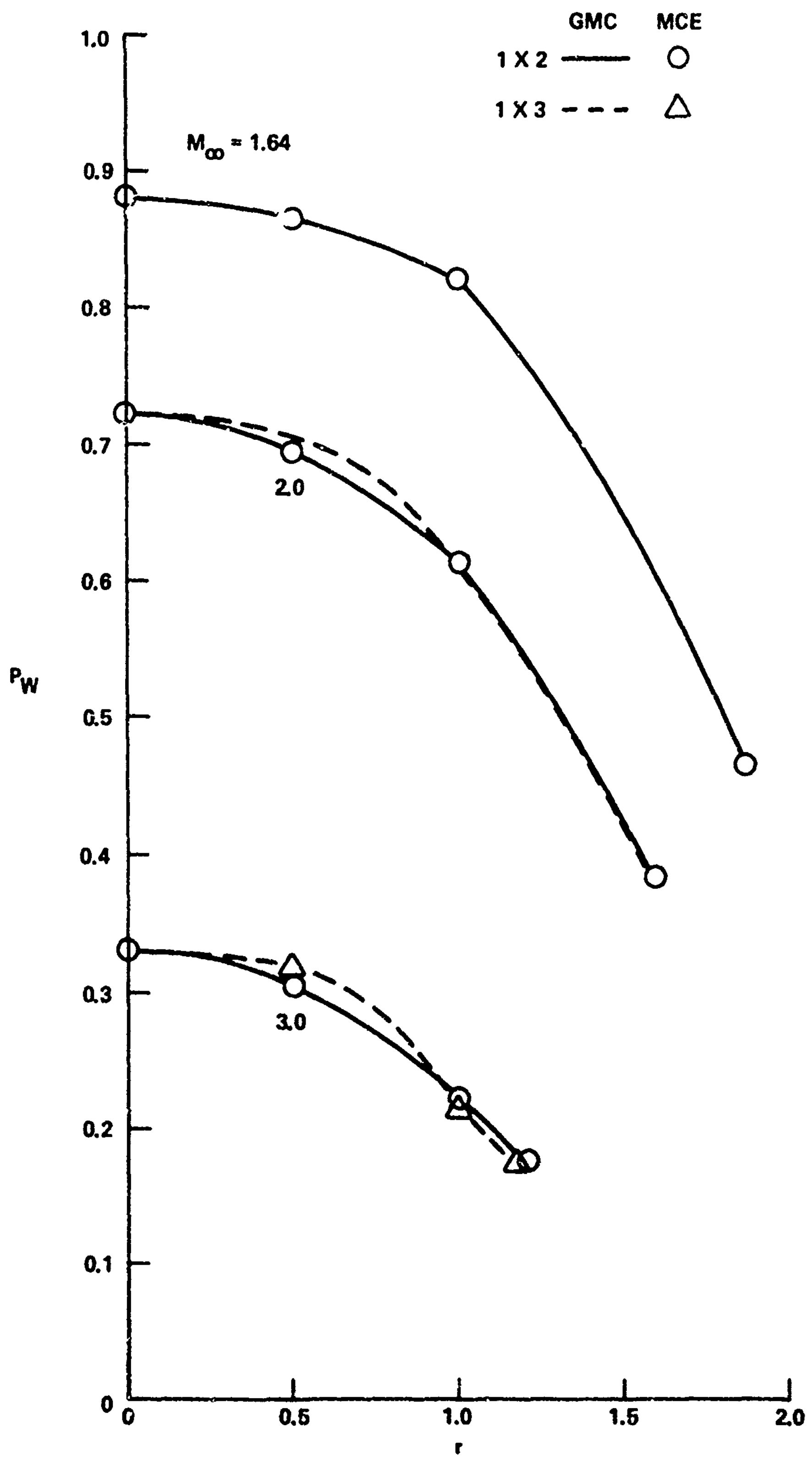

FIG. 11 SURFACE PRESSURE DISTRIBUTION: COMPARISON BETWEEN GMC AND MCE METHODS FOR PLANAR CASE

APPENDIX A

TWO-STRIP FORMULATION OF THE JET-IMPINGEMENT PROBLEM

METHOD OF INTEGRAL RELATIONS - SCHEME I

The flow field is divided into two strips in the axial (y-) direction by the middle line $y = \varepsilon/2$. The governing equations are different depending on whether they are in the shock layer $(0 \le r \le 1)$ or in the wall-jet layer $(1 \le r \le \eta)$.

A. SHOCK-LAYER REGION. Integrating the axial moment equation (2) from 0 to $\varepsilon/2$, we obtain

$$\frac{d}{dr}\int_0^{\varepsilon(r)/2} r^j \rho u v dy - \frac{1}{2}\frac{d\varepsilon}{dr} r^j \rho_H u_H v_H + r^j \Big\{ \beta(p_H - p_w) + \rho_H v_H^2 - \rho_w v_w^2 \Big\} = 0 \tag{A1}$$

where the subscript H denotes quantities evaluated at $y = \varepsilon/2$. If a quadratic profile in y is assumed for the integrands in Equations (A1) and (27), after some algebra, we may obtain, as an approximation to Equation (2), the following two ordinary differential equations:

$$\frac{d}{dr}(r^j \varepsilon \rho_s u_s v_s) + 4r^j \{\rho_s v_s (v_s + u_s \cot\sigma) - \rho_H v_H (2v_H + u_H \cot\sigma) + \beta(p_s - 2p_H + p_w)\} = 0 \tag{A2}$$

$$\frac{d}{dr}(r^j \varepsilon \rho_H u_H v_H) + \frac{r^j}{2} \{\rho_s v_s (v_s + u_s \cot\sigma) + 2\rho_H v_H (2v_H + u_H \cot\sigma) + \beta(p_s + 4p_H - 5p_w)\} = 0 \tag{A3}$$

Equations (5) and (17) have been used in the above equations. Similarly, Equations (1) and (3) yield

$$\frac{d}{dr}\left[r^j \varepsilon (\rho_w u_w - \rho_s u_s)\right] + 4r^j \{\rho_H (2v_H + u_H \cot\sigma) - \rho_s (v_s + u_s \cot\sigma)\} = 0 \tag{A4}$$

$$\frac{d}{dr}\left[r^j \varepsilon (2\rho_H u_H + \rho_s u_s)\right] + r^j \{5\rho_s (v_s + u_s \cot\sigma) - 2\rho_H (2v_H + u_H \cot\sigma)\} = 0 \tag{A5}$$

$$\frac{d}{dr}\left[r^j\varepsilon(\rho_w u_w^2 + \beta p_w - \rho_s u_s^2 - \beta p_s)\right] + 4r^j\{\rho_H u_H(2v_H + u_H\cot\sigma)$$

$$- \rho_s u_s(v_s + u_s\cot\sigma) + \beta(p_H - p_s)\cot\sigma\} = j\beta\varepsilon(p_w - p_s) \qquad \text{(A6)}$$

and

$$\frac{d}{dr}\left[r^j\varepsilon(\rho_s u_s^2 + \beta p_s + 2\rho_H u_H^2 + 2\beta p_H)\right] + r^j\{5\rho_s u_s(v_s + u_s\cot\sigma)$$

$$- 2\rho_H u_H(2v_H + u_H\cot\sigma) + \beta(5p_s - 2p_H)\cot\sigma\} = j\beta\varepsilon(2p_H + p_s) \qquad \text{(A7)}$$

The energy Equation (4) gives

$$p_w = \rho_w(1 - u_w^2) \qquad \text{(A8)}$$

and

$$p_H = \rho_H(1 - u_H^2 - v_H^2) \qquad \text{(A9)}$$

Thus, Equation (A2) defines the rate of change of σ, Equations (A4), (A6) and (A8) those of u_w, ρ_w and p_w, and Equations (A3), (A5), (A7) and (A9) those of u_H, v_H, ρ_H and p_H. Because of Equation (18), one may replace Equations (A6) and (A8) by the simpler algebraic relations, Equation (30) and

$$\rho_w = \left[\frac{1 - u_w^2}{E_{s0}}\right]^{1/(\gamma-1)} \qquad \text{(A10)}$$

Therefore, there are six ordinary differential equations (Eqs. (5), (A2) to (A5) and (A7)) for σ, ε, u_w, u_H, v_H and ρ_H. Initial conditions are, from Equations (19) to (21), at $r = 0$

$$u_{H0} = 0$$

$$u_{w0} = 0$$

$$\rho_{H0} = \left[\frac{(1 - v_{H0}^2)}{E_{s0}}\right]^{1/(\gamma-1)}$$

and

$$\sigma_0 = \pi/2$$

The two missing initial conditions for ε_0 and v_{H0} are supplied by the two regularity conditions at the surface sonic point and the singularity on the middle line. It is known for the jet-impingement problem that the surface sonic point, $r = \eta$, is outside the shock layer (Ref. (8)), but the location of the other "sonic" point on the middle line relative to the line of the jet edge ($r = 1$) is unknown a priori. These singularities and the associated regularity conditions, well-known for blunt-body problems, are essential for closing the system of equations. They will be discussed in detail later.

Because the structure of Equation (A2) is similar to Equation (28), Equation (A2) will also become singular as

$$\frac{d(\rho_s u_s v_s)}{d\sigma} = 0$$

and $d\sigma/dr$ will become unbounded. A formulation based on scheme III will thus be required. Before this, however, we shall complete the present discussion of the scheme I method by considering the wall-jet region.

B. <u>WALL-JET REGION</u>. Integrating Equations (1) to (3) from the plate to the middle line and from the plate to the upper boundary of the wall jet, and after some straightforward algebra, we obtain

$$\frac{d}{dr}(r^j \varepsilon \rho_j u_j v_j) + 4r^j\{\beta(p_j - 2p_H + p_w) - \rho_H v_H(2v_H + u_H \cot\delta)\} = 0 \quad \text{(A11)}$$

$$\frac{d}{dr}(r^j \varepsilon \rho_H u_H v_H) + \frac{r^j}{2}\{2\rho_H v_H(2v_H + u_H \cot\delta) + \beta(p_j + 4p_H - 5p_w)\} = 0 \quad \text{(A12)}$$

$$\frac{d}{dr}[r^j \varepsilon(\rho_w u_w - \rho_j u_j)] + 4r^j \rho_H(2v_H + u_H \cot\delta) = 0 \quad \text{(A13)}$$

$$\frac{d}{dr}[r^j \varepsilon(2\rho_H u_H + \rho_j u_j)] - 2r^j \rho_H(2v_H + u_H \cot\delta) = 0 \quad \text{(A14)}$$

$$\frac{d}{dr}\left[r^j \varepsilon(\rho_j u_j^2 + 2\rho_H u_H^2 + \beta p_j + 2\beta p_H)\right] + r^j\{\beta(5p_j - 2p_H)\cot\delta$$
$$- 2\rho_H u_H(2v_H + u_H \cot\delta)\} = j\beta\varepsilon(2p_H + p_j) \quad \text{(A15)}$$

As in the shock layer, the other ordinary differential equation that comes from the radial momentum equation (3) is replaced by the algebraic equations (30) and (A10). In addition, there is the geometric relation, Equation (6), the boundary conditions at the wall-jet boundary, Equations (8) to (16), and the energy equation (A9). Therefore, there are six ordinary differential equations (Eqs. (6), and (A11) to (A15)) for ε, δ, u_w, u_H, v_H and

ρ_H. Matching conditions at r = 1 supply the initial conditions. One may combine Equations (A13) and (A14) to give

$$r^j \varepsilon(\rho_w u_w + 4\rho_H u_H + \rho_j u_j) = \varepsilon_1(\rho_{w1} u_{w1} + 4\rho_{H1} u_{H1} + \rho_j u_{j1}) \quad \text{(A16)}$$

which, being an algebraic relation, can be used to replace, e.g., Equation (A14).

C. REGULARITY CONDITIONS. Utilizing Equation (A10) and after some straightforward algebra, we may rewrite Equation (A13) in the form

$$\frac{du_w}{dr} = \frac{N_1}{D_1}$$

where

$$D_1 \sim \left[1 - \left(\frac{\gamma + 1}{\gamma - 1}\right) u_w^2\right]$$

To have a finite value of du_w/dr at the singularity given by Equation (33), we require that $N_1 \to 0$ as $D_1 \to 0$ at $r = \eta$. This provides us with the regularity condition which, using Equation (A11) at $r = \eta$ to get rid of $d\delta_\eta/dr$ and after some straightforward algebra, becomes

$$q_j\left(\frac{j\varepsilon_\eta}{\eta} - \cot\delta_\eta\right)(\rho_{w\eta} u_{w\eta} \cos 2\delta_\eta + \rho_j q_j \sin^3\delta_\eta)$$

$$+ 4\rho_{H\eta}(2v_{H\eta} + u_{H\eta}\cot\delta_\eta)(q_j \cos 2\delta_\eta + v_{H\eta}\cos\delta_\eta)$$

$$- 4\beta\cos\delta_\eta(p_j - 2p_{H\eta} + p_{w\eta}) = 0 \quad \text{(A17)}$$

The location of the singularity on the middle line is again unknown a priori. Two different formulations are needed depending on whether it is larger than 1 or otherwise. Let's consider the first case (henceforth referred to as Case W), and denote the singularity to be at $r = \xi > 1$.

From Equations (A9), (A12), (A14) and (A15) we may obtain

$$\frac{du_H}{dr} = \frac{N_2}{D_2}$$

where

$$D_2 \sim (\gamma + 1)u_H^2 + (\gamma - 1)(v_H^2 - 1)$$

Therefore, as $D_2 \to 0$ at $r = \xi$, we need to impose the regularity condition that $N_2 \to 0$ at $r = \xi$. Using Equation (A11) at $r = \xi$ to get rid of $d\delta_\xi/dr$ (where the subscript ξ denotes quantities evaluated at ξ) and after some tedious but straightforward algebra, we may obtain the regularity condition

$$\rho_j q_j^2 \sin^2\delta_\xi [(\gamma - 1)\sin\delta_\xi - \gamma q_j u_{H\xi}] \left(\frac{j\varepsilon_\xi}{\xi} - \cot\delta_\xi\right)$$

$$+ \rho_{H\xi}(2v_{H\xi} + u_{H\xi}\cot\delta_\xi)\left[C_A(1 + 3v_{H\xi}^2 - u_{H\xi}^2) - 4C_B v_{H\xi}\right]$$

$$+ C_A u_{H\xi}\left[(2p_j - p_{H\xi})\cot\delta_\xi - \frac{j\varepsilon_\xi}{\xi} p_{H\xi}\right] + \beta[4C_B(p_j - 2p_{H\xi}$$

$$+ p_{w\xi}) + C_A v_{H\xi}(p_j + 4p_{H\xi} - 5p_{w\xi})] = 0 \qquad \text{(A18)}$$

where

$$C_A = (\gamma - 1)q_j \cos 2\delta_\xi$$

$$C_B = (1 - \gamma + 2\gamma q_j u_{H\xi}\sin\delta_\xi)\cos\delta_\xi$$

and , at $r = \xi$

$$u_{H\xi} = \left[\left(\frac{\gamma - 1}{\gamma + 1}\right)\left(1 - v_{H\xi}^2\right)\right]^{1/2} \qquad \text{(A19)}$$

It is easy to show that Equation (A19) is equivalent to $u_{H\xi} = a_{H\xi}$.

Let us now consider the case when the singularity on the middle line occurs in the shock layer. Henceforth, we shall refer to this case as Case S and denote the singularity to be at $r = \zeta < 1$. From Equations (A3), (A5), (A7) and (A9) we may obtain

$$\frac{du_H}{dr} = \frac{N_3}{D_3}$$

where again

$$D_3 \sim (\gamma + 1)u_H^2 + (\gamma - 1)(v_H^2 - 1)$$

This is to be expected since the structure of the governing equations in both layers is similar. Therefore, as $D_3 \to 0$ at $r = \zeta$, $N_3 \to 0$. Using Equation (A2) at $r = \zeta$ to get rid of $d\sigma_\zeta/dr$ (where the subscript ζ denotes quantities evaluated at $r = \zeta$) and after some tedious but straightforward algebra, we obtain, at $r = \zeta$

$$u_{H\zeta} = \left[\left(\frac{\gamma - 1}{\gamma + 1}\right)\left(1 - v_{H\zeta}^2\right)\right]^{1/2} \tag{A20}$$

and

$$\left[\frac{d(\rho_s u_s v_s)}{d\sigma}\right] \left\{\left[u_H(\beta p_s + \rho_s u_s^2) - 2\beta\rho_s u_s\right] \left(\frac{j\varepsilon}{r} - \cot\sigma\right)\right.$$

$$+ \rho_s(v_s + u_s\cot\sigma)[5u_s u_H + 2\beta(v_s v_H - 5)] + 2\beta\rho_H(2v_H + u_H\cot\sigma)$$

$$(1 + 3v_H^2 - u_H^2) + \beta(5p_s - 2p_H)u_H\cot\sigma + 2\beta^2 v_H(p_s + 4p_H - 5p_w)$$

$$\left. - j\beta u_H\varepsilon(2p_H + p_s)/r\right\} - \left[\beta u_H \frac{dp_s}{d\sigma} + u_H \frac{d(\rho_s u_s^2)}{d\sigma} - 2\beta \frac{d(\rho_s u_s)}{d\sigma}\right]$$

$$\left\{\rho_s u_s v_s\left(\frac{j\varepsilon}{r} - \cot\sigma\right) + 4[\rho_s v_s(v_s + u_s\cot\sigma) - \rho_H v_H(2v_H\right.$$

$$\left. + u_H\cot\sigma) + \beta(p_s - 2p_H + p_w)]\right\} = 0 \tag{A21}$$

where Equation (A21) is evaluated at $r = \zeta$.

D. STAGNATION-POINT VELOCITY GRADIENT. Dividing Equation (A2) by r^j and taking the limit as $r \to 0$, we obtain

$$(1 + j)\rho_{s0}v_{s0}\varepsilon_0\left(\frac{du_s}{dr}\right)_0 + 4\left\{\rho_{s0}v_{s0}^2 - 2\rho_{H0}v_{H0}^2\right.$$

$$\left. + \beta(p_{s0} - 2p_{H0} + p_{w0})\right\} = 0$$

Similarly, Equation (A4) yields

$$(1 + j)\varepsilon_0\left\{\rho_{w0}\left(\frac{du_w}{dr}\right)_0 - \rho_{s0}\left(\frac{du_s}{dr}\right)_0\right\} + 4(2\rho_{H0}v_{H0} - \rho_{s0}v_{s0}) = 0$$

Eliminating $(du_s/dr)_0$ from the above two equations we obtain

$$\left(\frac{du_w}{dr}\right)_0 = \frac{4[2\rho_{H0}v_{H0}(v_{H0} - v_{s0}) - \beta(p_{s0} - 2p_{H0} + p_{w0})]}{(1 + j)\rho_{w0}v_{s0}\varepsilon_0} \tag{A22}$$

for fixed values of M_∞ and γ, Equation (A22) indicates that the product $\varepsilon_0(du_w/dr)_0$ depends also on v_{H0}.

METHOD OF INTEGRAL RELATIONS - SCHEME III

A two-by-four formulation will be presented as an example below. To extend the formulation to two-by-n with n > 4 is straightforward, but the algebra involved will be much more complicated. In addition, there will be more equations to solve. This certainly will aggravate the convergence problem. For simplicity, we shall only present the details of Case W. The other case is very similar.

The flow field is divided in the radial direction into $(0, \frac{1}{2}, 1, \xi, \eta)$. In the shock layer, Equations (48) to (50) obviously still hold. In addition, Equations (A2) to (A5) are of the form of Equation (51), and hence they can be put into the forms of Equations (52) and (53), with the integrals and coefficients given by Equations (52a) to (53d). Equation (A7) is of the form

$$\frac{df}{dr} + r^j g = jh \tag{A23}$$

where g and h are, respectively, odd and even in r. In addition, $g_0 = 0$. Straightforward integrations of Equation (A23) over r yield

$$f_2 - f_0 + \int_0^{1/2} r^j g dr = j\int_0^{1/2} h dr \tag{A24}$$

and

$$f_1 - f_0 + \int_0^{1} r^j g dr = j\int_0^{1} h dr \tag{A25}$$

Consider the continuous approximating functions for g and h as

$$g \simeq \frac{r}{3}[8g_2 - g_1 + 4(g_1 - 2g_2)r^2]$$

$$h \simeq h_0 + \frac{(16h_2 - h_1 - 15h_0)}{3} r^2 + \frac{4(3h_0 + h_1 - 4h_2)}{3} r^4$$

Equations (A24) and (A25) become

$$f_k - f_0 + \sum_{i=0}^{2} (a_{ki}g_i - b_{ki}h_i) = 0 \quad , \quad k = 1,2 \tag{A26a,b}$$

where

$$a_{10} = a_{20} = 0$$

$$a_{11} = \frac{(3j + 4)}{3(j + 2)(j + 4)}$$

$$a_{12} = \frac{16}{3(j + 2)(j + 4)}$$

$$a_{21} = \frac{-2^{-(j+1)}}{3(j+2)(j+4)}$$

$$a_{22} = \frac{2^{-(j+1)}(3j+14)}{3(j+2)(j+4)}$$

$$b_{10} = \frac{2j}{15}$$

$$b_{11} = \frac{7j}{45}$$

$$b_{12} = \frac{32j}{45}$$

$$b_{20} = \frac{19j}{60}$$

$$b_{21} = \frac{-j}{180}$$

and

$$b_{22} = \frac{17j}{90}$$

In the wall-jet layer, consider

$$-\frac{d\varepsilon}{dr} = \cot\delta \simeq r\left[\frac{(\eta^2 - r^2)(\xi^2 - r^2)}{(\eta^2 - 1)(\xi^2 - 1)}\cot\delta_1 + \frac{(\xi^2 - r^2)(1 - r^2)}{\eta(\xi^2 - \eta^2)(1 - \eta^2)}\cot\delta_\eta + \frac{(\eta^2 - r^2)(1 - r^2)}{\xi(\eta^2 - \xi^2)(1 - \xi^2)}\cot\delta_\xi\right] \tag{A27}$$

Direct integration yields

$$\varepsilon = \varepsilon_1 - \frac{(r^2 - 1)}{12}\left\{\frac{\cot\delta_1}{(\eta^2 - 1)(\xi^2 - 1)}[6\eta^2\xi^2 - 3(\eta^2 + \xi^2)(r^2 + 1) + 2(r^4 + r^2 + 1)] + \frac{\cot\delta_\eta}{\eta(\xi^2 - \eta^2)(1 - \eta^2)}[6\xi^2 - 3(\xi^2 + 1)(r^2 + 1) + 2(r^4 + r^2 + 1)] + \frac{\cot\delta_\xi}{\xi(\eta^2 - \xi^2)(1 - \xi^2)}[6\eta^2 - 3(\eta^2 + 1)(r^2 + 1) + 2(r^4 + r^2 + 1)]\right\} \tag{A28}$$

After some algebra, we obtain

$$\varepsilon_\xi = \varepsilon_1 - \frac{(\xi^2 - 1)}{12}\left\{\frac{\cot\delta_1}{(\eta^2 - 1)}(3\eta^2 - \xi^2 - 2) - \frac{\cot\delta_\eta}{\eta(\xi^2 - \eta^2)(1 - \eta^2)}(\xi^2 - 1)^2 - \frac{\cot\delta_\xi}{\xi(\eta^2 - \xi^2)}(2\xi^2 - 3\eta^2 + 1)\right\} \tag{A29}$$

and ε_η is obtained by interchanging ξ and η in Equation (A29).

Equations (A11) to (A14) are of the form of Equation (51). The even function g can now be approximated again by the Lagrangian interpolation formula

$$g \approx \frac{(\eta^2 - r^2)(\xi^2 - r^2)}{(\eta^2 - 1)(\xi^2 - 1)} g_1 + \frac{(\xi^2 - r^2)(1 - r^2)}{(\xi^2 - \eta^2)(1 - \eta^2)} g_\eta + \frac{(\eta^2 - r^2)(1 - r^2)}{(\eta^2 - \xi^2)(1 - \xi^2)} g_\xi \tag{A30}$$

which is symmetric in ξ and η, i.e., the equation is unchanged by interchanging ξ and η. Integrating Equation (51) over r and using Equation (A30), we obtain

$$f_a - f_1 + g_1 G(\eta,\xi,1\ ;\ a) + g_\eta G(1,\xi,\eta\ ;\ a) + g_\xi G(1,\eta,\xi\ ;\ a) = 0 \quad ; \quad a = \xi,\eta \tag{A31a,b}$$

where

$$G(x,y,z\ ;\ r) \equiv \frac{S_j(x,y;r)}{(x^2 - z^2)(y^2 - z^2)} \tag{A32}$$

and

$$S_j(x,y;r) = \frac{x^2y^2}{(j + 1)}\left[r^{(j+1)} - 1\right] - \frac{(x^2 + y^2)}{(j + 3)}\left[r^{(j+3)} - 1\right] + \left[\frac{r^{(j+5)} - 1}{j + 5}\right] \tag{A33}$$

Equation (A15) is of the form of Equation (A23). Using Lagrangian interpolation formula for approximating the odd and even functions g and h, respectively, we obtain by straightforward integration

$$f_a - f_1 + g_1 H(\eta,\xi,1\ ;\ a) + g_\eta H(1,\xi,\eta;\ a) + g_\xi H(1,\eta,\xi\ ;\ a) =$$

$$j[h_1 K(\eta,\xi,1\ ;\ a) + h_\eta K(1,\xi,\eta\ ;\ a) + h_\xi K(1,\eta,\xi\ ;\ a)]\quad ;\quad a = \xi,\eta \tag{A34a,b}$$

where

$$H(x,y,z\ ;\ r) \equiv \frac{S_{j+1}(x,y\ ;\ r)}{z(x^2 - z^2)(y^2 - z^2)} \tag{A35}$$

and

$$K(x,y,z\ ;\ r) \equiv \frac{S_0(x,y\ ;\ r)}{(x^2 - z^2)(y^2 - z^2)} \tag{A36}$$

There are 22 basic unknowns in the two-by-four formulation: ε_0, ε_2 ε_1, δ_ξ, δ_η, u_{w2}, u_{w1}, $u_{w\xi}$, v_{H0}, v_{H2}, v_{H1}, $v_{H\xi}$, $v_{H\eta}$, u_{H2}, u_{H1}, $u_{H\eta}$, ρ_{H2}, ρ_{H1}, $\rho_{H\xi}$, $\rho_{H\eta}$, ξ and η. The basic equations are: Equations (A2) to (A5) in the forms of Equations (52) and (53); Equation (A7) in the forms of Equations (A26a,b); Equations (A11) to (A14) in the forms of Equations (A31a,b); Equation (A15) in the form of Equations (A34a,b); and the regularity conditions, Equations (A17) and (A18). Total number of equations is also 22 and the system is closed.

FLIGHT MEASUREMENTS DIVISION

EXTERNAL DISTRIBUTION LIST (A-1)

Copies

Commander, Naval Sea
Systems Command, Hqs.
Department of the Navy
Washington, D. C. 20360
Chief Tech. Analyst
SEA 05121
SEA 033
SEA 031
SEA 09G32 2
SEA 035

Commander, Naval Air Systems
Command, Hqs.
Department of the Navy
Washington, D. C. 20360
AIR 03B
AIR 03C
AIR 320
AIR 320C
Dr. H. J. Mueller, AIR 310
AIR 50174 2

Office of Navy Research
800 N. Quincy St.
Arlington, Va. 22217
ONR 100
Morton Cooper, 430B 2

Commander
Naval Ship Research and
Development Center
Bethesda, Md. 20035
Central Library Br. (5641)
Aerodynamics Lab. (5643)

Commander, Naval Weapons Center
China Lake, Calif. 93555
Technical Lib. (533)
Code 406
R. E. Meeker (4063)

Director, U. S. Naval
Research Laboratory
Washington, D. C. 20390
Library
Code 6503

NASA
Langley Research Center
Hampton, Va. 23665
MS/185 Technical Library
Aero & Space Mech. Div.
Dennis Bushnell
Ivan Beckwith
R. Trimpi
Julius Harris

NASA
Lewis Research Center
21000 Brookpart Road
Cleveland, Ohio 44135
Library 60-3
Ch, Wind Tunnel & Flight Div.

NASA
George C. Marshall Space
Flight Center
Huntsville, Ala. 35812
Mr. T. Reed, R-AERO-AU
Mr. W. K. Dahm,

NASA
600 Independence Ave., S. W.
Washington, D. C. 20546
F. C. Schwenk, Director,
Research (Code RR)

Copies

NASA
P. O. Box 33
College Park, Md. 20740

NASA Ames Research C
Moffett Field, Ca. 94035
Dr. M. Horstman
P. Kutler
J. Rakich
R. MacCormack
L. H. Jorgensen
E. J. Hopkins
H. H. Album
E. R. Keener

Technical Library
Director Defense Research and
Engineering (DDR+E)
Room 3E-1063, The Pentagon
Washington, D. C. 20301
Stop 103

Defense Documentation Center
Cameron Station
Alexandria, Va. 22314 12

Commander (5632.2)
Naval Missile Center
Point Mugu, Ca. 93041
Technical Library

Commanding Officer
USA Aberdeen Research and
Development Center
Aberdeen Proving Ground,
Maryland 21005
STEAP-TL (Tech Lib Div)
AMXRD-XSE

Director, Stragetic Systems
Project Office
Department of the Navy
Washington, D. C. 20390
SP-2722

Director of Intelligence
Hdqs., USAF (AFNINDE)
Washington, D. C. 20330
AFOIN-3B 2

Los Angeles Air Force Station
SAMSO/DYAE
P.O. Box 92960, Worldway Postal Center
Los Angeles, CA 90009
Code PSSE
Code RSSM

Headquarters, Arnold Engineering
Development Center
Arnold Air Force Station, Tenn. 37389
Library Documents
R. W. Henzel, .D
Capt. C. Tirres/DYR
C. Welsh

von Karman Gas Dynamics Facility
ARO, Inc.
Arnold Air Force Station, Tenn. 37389
Dr. J. Whitfield, Chief
L. M. Jenke
W. B. Baker, Jr.

DISTRIBUTION (CONT'D)

	Copies
Commanding Officer, Harry Diamond Laboratories Washington, D. C. 20438 Library, Rm 211, Bldg. 92	
Commanding General U. S. Army Missile Command Redstone Arsenal, Ala. 35809 AMSMI-RR Ch, Document Sec. AMSMI-RDK, Mr. R. Deep AMSMI-RDK, Mr. T. Street D. J. Spring	 2
Department of the Army Office of the Chief of Research and Development ABMDA, The Pentagon Washington, D. C. 20350	
Commanding Officer Picatinny Arsenal Dover, N. J. 07801 Mr. A. A. Loeb SMUPA-VC-3	
Commander (ADL) Naval Air Development Center Johnsville, Pa. 18974	
Air Force Weapons Laboratory Kirtland Air Force Base Albuquerque, N. M. 87117 Technical Library (SUL) Capt. Tolman/SAS	
U. S. Army Ballistic Missile Defense Agency 1300 Wilson Blvd. Arlington, Va. 22209 Dr. S. Alexander	
The Johns Hopkins University (C/NOw 7386) Applied Physics Laboratory 8621 Georgia Ave. Silver Spring, Md. 20910 Document Library Dr. F. Hill Dr. L. Cronvich	 2
Director, Defense Nuclear Agency Headquarters DASA Washington, D. C. 20305 STSP (SPAS)	
Commanding Officer Naval Intelligence Support Center 4301 Suitland Road Washington, D. C. 20390	
Department of Aeronautics DFAN USAF Academy Colorado 80840 Col. D. H. Daley Capt. J. Williams	
Armament Development and Test Center Eglin AFB, Fla. Technical Lib, DLOSL	
Headquarters, Edgewood Arsenal Edgewood Arsenal, Md. 21010 A. Flatau	

	Copies
Commander U. S. Army Natick Development Center Natick, Mass. 01760 AMXNM-UBS G. A. Barnard	
AFFDL/FX Wright-Patterson Air Force Base Dayton, Ohio 45433 Dr. D. J. Harney	
AFFDL/FXG Wright-Patterson Air Force Base Dayton, Ohio 45433 Mr. M. Buck P. Giragosian	
Naval Air Test Facility Lake Hurst, N. J. 08733 Dr. W. Sule	
Army Aviation Systems Command P. O. Box 209, Main Office St. Louis, Mo. 63166 Dr. L. Lijewski	

EXPERIMENTAL AERODYNAMICS BRANCH

EXTERNAL DISTRIBUTION LIST (A2)

Copies

Aerospace Engineering
Program
University of Alabama
P. O. Box 2908
University, Alabama 35406
Prof. W. K. Rey, Chm.

AME Department
University of Arizona
Tucson, Arizona 85721
Dr. L. B. Scott

Polytechnic Institute of
Brooklyn
Graduate Center Library
Route 110, Farmingdale
Long Island, New York 11735
Dr. J Polczynski

Polytechnic Institute of
Brooklyn
Spicer Library
333 Jay Street
Brooklyn, New York 11201
Reference Department

California Institute of
Technology
Pasadena, CA 91109
Graduate Aeronautical Labs.
Aero. Librarian
Prof. D. Coles, 321
Guggenheim Lab.
Dr. A. Roshko

University of California
Dept. of Mechanical Engineering
Berkeley, CA 94720
Prof. R. Grief

Notre Dame University
Notre Dame, Indiana 46556
Dr. V. Goddard
Dr. V. Nee
Dr. T. Muller
Dr R. Nelson
Dr. F. Raven
Prof. R. Eikenberry
Dept of Aero Eng., College of Engr.
Library

GASDYNAMICS
University of California
Richmond Field Station
1301 South 46th Street
Richmond, California 94804
A. K. Oppenheim

Department of Aerospace
Engineering
University of Southern
California
University Park
Los Angeles
California 90007
Dr. John Laufer

University of California -
San Diego
Department of Aerospace and
Mechanical Engineering
Sciences
LaJolla, California 92037
Dr. P. A. Libby

Copies

Case Western Reserve
University
Division of Fluid, Thermal
and Aerospace Engineering
Cleveland, Ohio 44106
Dr. Eli Reshotko, Head

The Catholic University of
America
Washington, D.C. 20017
Dr. C. C. Chang
Dr. Paul K. Chang
Mechanical Engr. Dept.
Dr. M. J. Casarella
Mechanical Engr. Dept.

University of Cincinnati
Cincinnati, Ohio 45221
Department of Aerospace
Engineering
Dr. Arnold Polak

Department of Aerospace
Engineering Sciences
University of Colorado
Boulder, Colorado 80302

Cornell University
Graduate School of Aero.
Engineering
Ithaca, New York 14850
Prof W. R. Sears
Dr. S. F. Shen
Prof. F. K. Moore, Head
Thermal Engineering
Dept., 208 Upson Hall

University of Delaware
Mechanical and Aeronautical
Engineering Dept.
Newark, Delaware 19711
Dr. James E. Danberg

Georgia Institute of
Technology
225 North Avenue, N.W.
Atlanta, Georgia 30332
Dr. Arnold L. Ducoffe

Technical Reports
Collection
Gordon McKay Library
Harvard University
Div. of Eng'g. and
Applied Physics
Pierce Hall
Oxford Street
Cambridge
Massachusetts 02138

Illinois Institute of
Technology
3300 South Federal
Chicago, Illinois 60616
Dr. M. V. Morkovin
Prof. A. A. Fejer
M.A.E. Dept.

University of Illinois
101 Transportation Bldg.
Urbana, Illinois 61801
Aeronautical and
Astronautical
Engineering Dept.

Iowa State University
Ames, Iowa 50010
Aerospace Engineering
Dept.

DISTRIBUTION (CONT)

Copies

The Johns Hopkins University
Baltimore, Maryland 21218
Prof. S. Corrsin

University of Kentucky
Wenner-Gren Aero. Lab.
Lexington, Kentucky 40506
C. F. Knapp

Department of Aero.
Engineering, ME 106
Louisianna State University
Baton Rouge
Louisiana 70803
Dr. P. H. Miller

University of Maryland
College Park
Maryland 20740
Prof. A. Wiley Sherwood
Department of Aerospace
Engineering
Prof. Charles A. Shreeve
Department of
Mechanical Engineering
Dr. S. I. Pai, Institute
for Fluid Dynamics and
Applied Mathematics
Dr. Redfield W. Allen
Department of
Mechanical Engineering
Dr. W. L. Melnik
Department of
Aerospace Engineering
Dr. John D. Anderson, Jr.
Department of
Aerospace Engineering

Michigan State University
Library
East Lansing
Michigan 48823
Documents Department

Massachusetts Institute of
Technology
Cambridge
Massachusetts 02139
Mr. J. R. Martuccelli
Rm. 33-211
Prof. M. Finston
Prof. J. Baron, Dept.
of Aero. and Astro.
Rm. 37-461
Prof. A. H. Shapiro
Head, Mech. Engr. Dept.
Aero. Engineering Library
Prof. Ronald F. Probstein
Dr. E. E. Covert
Aerophysics Laboratory

University of Michigan
Ann Arbor, Michigan 48104
Dr. M. Sichel, Dept of Aero Engr
Engineering Library
Aerospace Engineering Lib.
Mr. C. Cousineau, Engin-Trans Lib.

Serials and Documents
Section
General Library
University of Michigan
Ann Arbor, Michigan 48104

Mississippi State
University
Department of Aerophysics
and Aerospace Engineering
P.O. Drawer A
State College, Mississippi 39762
Mr. Charles B. Cliett

Copies

U.S. Naval Academy
Annapolis, Maryland 21402
Engineering Department
Aerospace Division

Library, Code 2124
U. S. Naval Postgraduate
School
Monterey, California 93940
Technical Reports Section

New York University
University Heights
New York, New York 10453
Dr. Antonio Ferri
Director of Guggenheim
Aerospace Laboratories
Prof. V. Zakkay
Engineering and Science
Library

North Carolina State College
Raleigh
North Carolina 27607
Dr. F. R. DeJarnette, Dept
Mech. and Aero.
Engineering
Dr. H. A. Hassan, Dept. of
Mech. and Aero. Engr.

D. H. Hill Library
North Carolina State
University
P.O. Box 5007
Raleigh
North Carolina 27607

University of North Carolina
Chapel Hill
North Carolina 27514
Department of Aero.
Engineering
Library, Documents Section
AFROTC Det 390

Northwestern University
Technological Institute
Evanston, Illinois 60201
Department of Mechanical
Engineering
Library

Virginia Polytechnical Institute
Blacksburg, Va. 24061
Prof. G. Inger

Department of Aero-Astro
Engineering
Ohio State University
2036 Neil Avenue
Columbus, Ohio 43210
Engineering Library
Prof. J. D. Lee
Prof. G. L. Von Eschen

Ohio State University
Libraries
Documents Division
1858 Neil Avenue
Columbus, Ohio 43210

The Pennsylvania State
University
University Park
Pennsylvania 16802
Dept. of Aero Engr.
Hammond Bldg.
Library, Documents
Section

Bevier Engineering Library
126 Benedum Hall
University of Pittsburgh
Pittsburgh
Pennsylvania 15261

DISTRIBUTION (CONT)

COPIES

Princeton University
Aerospace and Mechanical Science Dept.
D-2 Engrg. Quadrangle
Princeton
New Jersey 08540
Prof. S. Bogdonoff
Dr. I. E. Vas

Purdue University
School of Aeronautical and Engineering Sciences
Lafayette, Indiana 47907
Library
Dr. B. Reese, Head, Dept of Aero. & Astro.

Rensselaer Polytechnic Institute
Troy, New York 12181
Dept. of Aeronautical Engineering and Astronautics

Department of Mechanical Industrial and Aerospace Engineering
Rutgers - The State University
New Brunswick, N. J. 08903
Dr. R. H. Page
Dr. C. F. Chen

Stanford University
Stanford
California 94305
Librarian, Dept. of Aeronautics and Astronautics

Stevens Institute of Technology
Hoboken, New Jersey 07030
Mechanical Engineering Department
Library

The University of Texas at Austin
Applied Research Laboratories
P. O. Box 8029
Austin, Texas 78712
Director
Engr S.B.114B/Dr. Friedrich

University of Toledo
2801 W. Bancroft
Toledo, Ohio 43606
Dept. of Aero Engineering
Dept. of Mech Engineering

University of Virginia
School of Engineering and Applied Science
Charlottesville
Virginia 22901
Dr. I. D. Jacobson
Dr. G. Matthews
Dr. R. N. Zapata

University of Washington
Seattle
Washington 98105
Engineering Library
Dept. of Aeronautics and Astronautics
Prof. R. E. Street, Dept. of Aero. and Astro.
Prof. A. Hertzberg, Aero. and Astro., Guggenheim Hall

West Virginia University
Morgantown
West Virginia 26506
Library

COPIES

Federal Reports Center
University of Wisconsin
Mechanical Engineering Building
Madison, Wisconsin 53706
S. Reilly

Prototype Development Associates
1740 Garry Avenue
Suite 201
Santa Ana, CA 92705
Dr. J. Dunn
Dr. P. Crenshaw

Los Alamos Scientific Laboratory
P.O. Box 1663
Los Alamos
New Mexico 87544
Report Library

University of Maryland
Baltimore County (UMBC)
5401 Wilkens Avenue
Baltimore, Maryland 21228
Dr. R. C. Roberts
Mathematics Department

Systems Research Laboratories, Inc.
2800 Indian Ripple Road
Dayton, Ohio 45440
Dr. K. Ball
Dr. C. Ingram

Institute for Defense Analyses
400 Army-Navy Drive
Arlington, Virginia 22202
Classified Library

Kaman Sciences Corporation
P.O. Box 7463
Colorado Springs
Colorado 80933
Library

Kaman Science Corporation
Avidyne Division
83 Second Avenue
Burlington
Massachusetts 01803
Dr. J. R. Ruetenik

Rockwell International
B-1 Division
Technical Information Center (BA08)
International Airport
Los Angeles, Ca. 90009

Rockwell International Corporation
Technical Information Center
4300 E. Fifth Avenue
Columbus, Ohio 43216

M. I. T. Lincoln Laboratory
P.O. Box 73
Lexington
Massachusetts 02173
Library A-082

The RAND Corporation
1700 Main Street
Santa Monica
California 90406
Library - D

Aerojet Electrosystems Co.
1100 W. Hollyvale Ave.
Azusa, Ca. 91702
Engineering Library

DISTRIBUTION (CONT)

Copies

The Boeing Company
P.O. Box 3999
Seattle, Washington 98124
87-C7

United Aircraft
Research Laboratories
East Hartford
Connecticut 06108
Dr. William M. Foley

United Aircraft Corporation
400 Main Street
East Hartford
Connecticut 06108
Library

Hughes Aircraft Company
Centinela at Teale
Culver City, Ca. 90230
Company Tech. Doc. Center
6/E11, B. W. Campbell

Lockheed Missiles & Space Co.
Continental Bldg., Suite 445
El Segundo, CA 90245
T. R. Fortune
F. E. Huggin

Lockheed Missiles and Space
Company
P.O. Box 504
Sunnyvale
California 94086
Mr. G. M. Laden, Dept.
81-25, Bldg. 154
Mr. Murl Culp

Lockheed Missiles and Space
Company
3251 Hanover Street
Palo Alto, California 94304
Technical Information
Center

Lockheed-California
Company
Burbank, California 91503
Central Library, Dept.
84-40, Bldg. 170
PLT. B-1

Vice President and Chief
Scientist
Dept. 03-10
Lockheed Aircraft
Corporation
P.O. Box 551
Burbank, California 91503

Martin Marietta Corporation
P.O. Box 988
Baltimore
Maryland 21203
Science-Technology Library
(Mail No. 398)

Martin Company
3211 Trade Winds Trail
Orlando, Florida 32805
Mr. H. J. Dicholt

General Dynamics
P.O. Box 748
Fort Worth, Texas 76101
Research Library 2246
George Kaler, Mail Zone
2880

Copies

Calspan Corporation
4455 Genesee Street
Buffalo, New York 14221
Library

Air University Library
(SE) 63-578
Maxwell Air Force Base
Alabama 36112

McDonnell Company
P.O. Box 516
St. Louis, Missouri 63166
R. D. Detrich, Dept. 209
Bldg. 33
W. Brian Brooks

McDonnell Douglas Astronautics Co. - West
5301 Bolsa Avenue
Huntington Beach, California 92647
A3-339 Library
J. S. Murphy, A3-833
M. Michael Briggs

Fairchild Hiller
Republic Aviation Division
Farmingdale
New York 11735
Engineering Library

General Applied Science
Laboratories, Inc.
Merrick and Stewart
Avenues
Westbury, Long Island
New York 11590
Dr. F. Lane
L. M. Nucci

General Electric Company
Research and Development
Lab. (Comb. Bldg.)
Schenectady
New York 12301
Dr. H. T. Nagamatsu

The Whitney Library
General Electric Research
and Development Center
... Knolls, K-1
P.O. Box 8
Schenectady
New York 12301
M. F. Orr, Manager

General Electric Company
Missile and Space Division
P.O. Box 8555
Philadelphia
Pennsylvania 19101
MSD Library
Larry Chasen, Mgr.
Dr. J. D. Stewart, Mgr.
Research and Engineering

General Electric Company
AEG Technical Information
Center, N-32
Cincinnati, Ohio 45215

General Electric Company
Re-Entry & Environmental Systems
Division
3198 Chestnut Street
Philadelphia, Penn. 19101
Dr. S. M. Scala
Dr. H. Lew
Mr. J. W. Faust
A. Martellucci
W. Daskin
J. D. Cresswell
J. Pettus
L. A. Marshall
J. Cassanto
R. Hobbs
C. Harris
F. George

DISTRIBUTION (CONT)

	Copies
AVCO-Everett Research Laboratory 2385 Revere Beach Parkway Everett Massachusetts 02149 Library Dr. George Sutton	2
LTV Aerospace Corporation Vought Aeronautics Division P.O. Box 5907 Dallas, Texas 75222 Unit 2-51131 (Library)	
LTV Aerospace Corporation Missiles and Space Division P.O. Box 6267 Dallas, Texas 75222 MSD-T-Library	
Northrop Norair 3901 West Broadway Hawthorne California 90250 Tech. Info. 3360-32	
Government Documents The Fondren Library Rice Institute P.O. Box 1892 Houston, Texas 77001	
Grumman Aircraft Engineering Corporation Bethpage, Long Island New York 11714 Mr. R. A. Scheuing Mr. H. B. Hopkins Mr. H. R. Reed	
Marquardt Aircraft Corporation 16555 Saticoy Street Van Nuys, California 91409 Library	
ARDE Associates P.O. Box 286 580 Winters Avenue Paramus, New Jersey 07652 Librarian	
Aerophysics Company 3500 Connecticut Ave., N.W. Washington, D.C. 20003 Mr. G. D. Boehler	
Aeronautical Research Associates of Princeton 50 Washington Road Princeton New Jersey 08540 Dr. C. duP. Donaldson	
General Research Corporation 5383 Hollister Avenue P.O. Box 3587 Santa Barbara California 93105 Technical Information Office	
Sandia Laboratories Mail Service Section Albuquerque, N. M. 87115 Mr. K. Goin, Div. 5262 Mr. W. H. Curry, Div. 1331 Mr. A. M. Tornsby, 3141 Dr. G. Stone Div. 3141	
Hercules Incorporated Allegany Ballistics Laboratory P.O. Box 210 Cumberland Maryland 21502 Library	

	Copies
General Electric Company P.O. Box 2500 Daytona Beach Florida 32015 Dave Hovis, Rm. 4109	
TRW Systems Group 1 Space Park Redondo Beach California 90278 Technical Libr//Doc Acquisitions B. Pearce, Aero Dept. F. D. Deffenbaugh	
Stanford Research Institute 333 Ravenswood Avenue Menlo Park California 94025 Dr. G. Abrahamson	
Hughes Aircraft Company P.O. Box 3310 Fullerton California 92634 Technical Library, 600-C222	
Westinghouse Electric Corporation Astronuclear Laboratory P.O. Box 10864 Pittsburgh Pennsylvania 15236 Library	
University of Tennessee Space Institute Tullahoma Tennessee 37388 Prof. J. M. Wu	
CONVAIR Division of General Dynamics Library and Information Services P.O. Box 12009 San Diego California 92112	
CONVAIR Division of General Dynamics Post Office Box 80986 San Diego, California 92138 Dr. J. Raat Mail Zone 640-02 Research Library	
AVCO Missiles Systems Division 201 Lowell Street Wilmington Massachusetts 01887 E. E. H. Schurmann J. Otis	
Chrysler Corporation Space Division P.O. Box 29200 New Orleans, La. 70189 N. D. Kemp, Dept. 2910 E. A. Rawls, Dept. 2920	
General Dynamics Pomona Division P.O. Box 2507 Pomona, Ca. 91766 Tech. Doc. Center, Mail Zone 6-20	
General Electric Company 3198 Chesnut Street Philadelphia, Pa. 19101 W. Danskin Larry Chasen Dr. H. Lew	
Philco-Ford Corporation Aeronutronic Division Newport Beach California 92660 Dr. A. Demetriades	

DISTRIBUTION (CONT)

Copies

Raytheon Company
Missile Systems Division
Hartwell Road
Bedford, Ma. 01730
D. P. Forsmo

TRW Systems Group
Space Park Drive
Houston, Texas 77058
M. W. Sweeney, Jr.

Marine Bioscience Laboratory
513 Sydnor Street
Ridgecrest, Ca. 93555
Dr. A. C. Charters

University of California - Los Angeles
Dept of Mechanics & Structures
Los Angeles, Ca. 90024
Prof. J. D. Cole

University of Wyoming
University Station
P. O. Box 3295
Laramie, Wyoming 82070
Head, Dept. Mech. Eng.

Applied Mechanics Review
Southwest Research Institute
8500 Culebra Road
San Antonio, Texas 78228

American Institute of Aeronautics and Astronautics
1290 Sixth Avenue
New York, New York 10019
J. Newbauer

Technical Information Service
American Institute of Aeronautics and Astronautics
750 Third Avenue
New York, New York 10017
Miss P. Marshall

Faculty of Aeronautical Systems
University of West Florida
Pensacola, Florida 32504
Dr. R. Fledderman

Space Research Corporation
Chittenden Bank Building
North Troy, Vermont 05859
Library
J. A. Finkel

The Aerospace Corporation
P. O. Box 92957
Los Angeles, California 90009
J. M. Lyons, Bldg. 82

Chrysler Corp., Defense Division
Detroit, Michigan 48231
Dr. R. Lusardi

AERO
3020 Buckingham Drive
South Bend, Indiana 46614
Dr. J. Nicolaides

Acurex Corp. Aerotherm
485 Clyde Avenue
Mt. View, CA 94042
L. Cooper

Sandia Corporation
Livermore, CA 94550
J. K. Kryvoruka

Copies

Near, Inc.
510 Clyde Avenue
Mountain View, CA 94043

CONVAIR Division of General Dynamics
P.O. Box 80847
San Diego, California 92138
Dr. E. S. Levinsky
Mail Zone 667-1